Hippocampal protein aggregation signatures fully distinguish pathogenic and wildtype *UBQLN2* in amyotrophic lateral sclerosis

Kyrah M. Thumbadoo[1,2], Birger V. Dieriks[2,3], Helen C. Murray[2,3], Molly E. V. Swanson[1,3], Ji Hun Yoo[2,4], Nasim F. Mehrabi[2,3], Clinton Turner[2,3,5], Michael Dragunow[2,4], Richard L. M. Faull[2,3], Maurice A. Curtis[2,3], Teepu Siddique[6], Christopher E. Shaw[2,7], Lyndal Henden[8], Kelly L. Williams[8], Garth A. Nicholson[8,9,10,11], Emma L. Scotter[1,2]

1 School of Biological Sciences, University of Auckland, Auckland, New Zealand
2 Centre for Brain Research, University of Auckland, Auckland, New Zealand
3 Department of Anatomy and Medical Imaging, University of Auckland, Auckland, New Zealand
4 Department of Pharmacology and Clinical Pharmacology, University of Auckland, Auckland, New Zealand
5 Department of Anatomical Pathology, LabPlus, Auckland City Hospital, Auckland, New Zealand
6 Departments of Neurology, Cell and Developmental Biology and Pathology, Northwestern University Feinberg School of Medicine, Chicago, USA
7 UK Dementia Research Institute Centre, Institute of Psychiatry, Psychology and Neuroscience, King's College London, United Kingdom
8 Macquarie University Centre for Motor Neuron Disease Research, Macquarie Medical School, Faculty of Medicine, Health and Human Sciences, Macquarie University, Sydney, New South Wales, Australia
9 Northcott Neuroscience Laboratory, Australian and New Zealand Army Corps (ANZAC) Research Institute, Concord, New South Wales, Australia
10 Faculty of Medicine, University of Sydney, Sydney, New South Wales, Australia
11 Molecular Medicine Laboratory, Concord Repatriation General Hospital, Concord, New South Wales, Australia

Corresponding author:
Email, emma.scotter@auckland.ac.nz; Telephone, +64 9 923 1350

Acknowledgements and funding

This publication is dedicated to the incredible patients and families who contribute to our research. We thank Marika Eszes at the Centre for Brain Research, University of Auckland, New Zealand; Nailah Siddique at the Northwestern University Feinberg School of Medicine, Chicago, USA; Sashika Selvaduncko and Claire Troakes at the London Neurodegenerative Diseases Brain Bank and Brains for Dementia; and the Neurological Foundation of New Zealand for their ongoing financial support of the Human Brain Bank. We also thank Fairlie Hinton and Dr. Catriona McLean at the Victorian Brain Bank, which is supported by The Florey Institute of Neuroscience and Mental Health, The Alfred and the Victorian Forensic Institute of Medicine and funded in part by Parkinson's Victoria, MND Victoria, FightMND and Yulgilbar Foundation. The imaging data reported in this paper were obtained at the Biomedical Imaging Research Unit (BIRU), operated by the Faculty of Medical and Health Sciences' Technical Services at the University of Auckland. KT was funded by a doctoral scholarship from Amelia Pais-Rodriguez and Marcus Gerbich. BVD and MD were funded by the Michael J Fox Foundation [Grant ID: 16420]. BVD was also funded by a Health Research Council Sir Charles Hercus Health Research Fellowship [21/034]. ELS was supported by Marsden FastStart and Rutherford Discovery Fellowship funding from the Royal Society of New Zealand [15-UOA-157, 15-UOA-003]. This work was also supported by grants from Motor Neuron Disease NZ, Freemasons Foundation of New Zealand, Matteo de Nora, Sir Thomas and Lady Duncan Trust and the Coker Family Trust (to MD), and PaR NZ Golfing. No funding body played any role in the design of the study, nor in the collection, analysis, or interpretation of data nor in writing the manuscript.

Authors' contributions

KMT, BVD, HCM, MEVS, JHY, NFM conducted or designed experiments; KMT, BVD, HCM, MEVS, ELS performed data analysis or designed analysis methods; CT conducted neuropathological diagnostics; MD provided study supervision and resourcing; RLMF, MAC, TS, CES coordinated the banking and use of human tissue for study; TS, CES, GAN identified the *UBQLN2* patients; KLW, LH performed relatedness analysis; KMT, BVD,

ELS wrote the manuscript; GAN, ELS conceived of the study. ELS designed the study. All authors read, edited, and approved the final manuscript.

Abstract

Mutations in the *UBQLN2* gene cause X-linked dominant amyotrophic lateral sclerosis (ALS) and/or frontotemporal dementia (FTD) characterised by ubiquilin 2 aggregates in neurons of the motor cortex, hippocampus, and spinal cord. However, ubiquilin 2 neuropathology is also seen in sporadic and familial ALS or FTD cases not caused by *UBQLN2* mutations, particularly *C9orf72*-linked cases. This makes the mechanistic role of ubiquilin 2 mutations and the value of ubiquilin 2 pathology for predicting genotype unclear. Here we examine a cohort of 41 genotypically diverse ALS cases with or without FTD, including five cases with *UBQLN2* variants (resulting in p.S222G, p.P497H, p.P506S, and two cases with p.T487I). Using multiplexed (5-label) fluorescent immunohistochemistry, we mapped the co-localisation of ubiquilin 2 with phosphorylated TDP-43 (pTDP-43), dipeptide repeat aggregates, and p62, in the hippocampus of controls (n=5), or ALS with or without FTD in sporadic (n=20), unknown familial (n=3), *SOD1*-linked (n=1), *FUS*-linked (n=1), *C9orf72*-linked (n=5), and *UBQLN2*-linked (n=5) cases. We differentiate between i) ubiquilin 2 aggregation together with pTDP-43 or dipeptide repeat proteins, and ii) ubiquilin 2 self-aggregation promoted by *UBQLN2* gene mutations that cause ALS/FTD. Overall, we describe a hippocampal protein aggregation signature that fully distinguishes mutant from wildtype ubiquilin 2 in ALS with or without FTD, whereby mutant ubiquilin 2 is more prone than wildtype to aggregate independently of driving factors. This neuropathological signature can be used to assess the pathogenicity of *UBQLN2* gene variants and to understand the mechanisms of *UBQLN2*-linked disease.

Keywords: *UBQLN2*, ubiquilin 2, amyotrophic lateral sclerosis (ALS), frontotemporal dementia (FTD), neuropathology, hippocampus, human, TDP-43, polyGP, polyGA

Introduction

UBQLN2 gene mutations are a rare cause of amyotrophic lateral sclerosis (ALS) with or without dementia, and the only known causal mutations on the X-chromosome. *UBQLN2* [NM_013444] encodes the ubiquilin 2 protein, the best studied of five human ubiquilins, which contains a unique PXX domain comprising 12 proline-rich tandem repeats [1,2]. Like other ALS- and FTD-linked degradation proteins (sequestosome 1/p62 (hereafter p62), valosin-containing protein, optineurin, and TANK-binding kinase 1), a key role for ubiquilin 2 is to bind ubiquitinated, misfolded, and aggregated protein cargos, triaging them between the proteasome and autophagy intracellular degradation pathways [3–6]. New evidence suggests that ubiquilin 2 is intrinsically prone to self-assembly and undergoes reversible liquid-liquid phase separation, allowing it to bind ubiquitin-labelled proteins within phase-separated stress granules. It is postulated that upon ubiquitinated protein binding, ubiquilin 2 comes out of the liquid-droplet phase, bringing its cargo from the stress granule for delivery to the proteasome; ubiquilin 2 is therefore also implicated in stress granule disassembly [7–10].

These roles at the interface between RNA processing and protein degradation — two key pathways in ALS and FTD pathogenesis — may underpin why ubiquilin 2 mutations cause disease. ALS and/or FTD (ALS/FTD)-causing *UBQLN2* mutations that alter residues flanking and within the PXX domain impair ubiquilin 2 binding to the proteasome and promote self-oligomerisation and liquid-to-solid rather than liquid-liquid phase transition [9,11–14]. The mutation c.1490C>A, resulting in p.P497H, was the first disease-causing *UBQLN2* mutation identified, leading to the discovery in unrelated ALS/FTD families of mutations c.1489C>T (p.P497S), c.1516C>A (p.P506T), c.1525C>T (p.P509S) and c.1573C>T (p.P525S) all altering the PXX domain [1]. A c.1516C>T mutation, resulting in p.P506S also within the PXX domain, was later identified in a family with young onset ALS, ALS with FTD onset, or pure spastic paraplegia [15] while a c.1460C>T mutation, resulting in p.T487I just upstream of the PXX region, was found in two families with members in New Zealand and Australia [16,17]. *UBQLN2* mutations/variants have also been identified in ALS/FTD cases altering other residues within or flanking the PXX domain; in the ubiquitin-like domain; the stress-induced protein 1-like domains; or outside

124 of known domains [18–37]. However, it is currently uncertain whether all of these
125 *UBQLN2* variants are pathogenic (disease-causing).
126
127 The neuropathology of ALS/FTD caused by pathogenic *UBQLN2* mutations is
128 characterised by aggregated ubiquilin 2 in the motor cortex, spinal cord, and hippocampus
129 [1,15,17,23,38]. We previously reported ubiquilin 2-positive aggregates in the
130 hippocampus of an individual with p.T487I *UBQLN2*-linked ALS+FTD, but not in
131 sporadic ALS [38]. However, ubiquilin 2 inclusions are not specific to *UBQLN2*-linked
132 ALS/FTD cases and have been identified previously in sporadic and familial ALS, and
133 ALS-dementia, regardless of whether ubiquilin 2 is wildtype or mutant [1,15,17,23,38,39].
134 Some of these ubiquilin 2 inclusions are immunopositive for other ALS/FTD-linked
135 proteins such as TDP-43 or phosphorylated TDP-43 (pTDP-43), FUS, p62, optineurin, or
136 ubiquitin [1,17,40–44]. In addition, deposition of ubiquilin 2 in the hippocampus is a
137 characteristic feature of ALS/FTD caused by *C9orf72* hexanucleotide repeat expansions,
138 in which ubiquilin 2 is seen in the presence of dipeptide repeat (DPR) proteins [39]. Thus,
139 while ubiquilin 2 is clearly involved in ALS/FTD pathogenesis regardless of aetiology, the
140 role of *UBQLN2* mutations and the predictive value of ubiquilin 2 labelling in relation to
141 genotype is still unclear.
142
143 There is a clear need to determine whether *UBQLN2* mutations cause ubiquilin 2
144 neuropathology that is distinct from the wildtype ubiquilin 2 neuropathology that is seen
145 in ALS/FTD with other genotypes. If they do, then defining a pathological signature for
146 *UBQLN2*-linked disease will provide mechanistic insights and aid assessment of the
147 pathogenicity of *UBQLN2* genetic variants which are not yet confirmed to be causative.
148 Because ubiquilin 2 aggregation across a range of ALS/FTD genotypes occurs in the
149 hippocampus, this region may provide insight into the requirements for mutant and
150 wildtype ubiquilin 2 aggregation. Here we map the hippocampal ubiquilin 2 protein
151 deposition signature with respect to pTDP-43, the two most abundant *C9orf72*-linked DPR
152 proteins, and p62, in ALS/FTD with and without *UBQLN2* mutation.

153 ## Materials and methods

154 **Systematic review of *UBQLN2*-linked ALS/FTD neuropathology**

155 Journal articles were identified using PubMed that were published between Jan 1993 and
156 May 2023. Search terms were *UBQLN2*, ubiquilin 2, amyotrophic lateral sclerosis, and
157 ALS, combined with neuropathology, tissue, or immunohistochemistry. Articles which did
158 not contain ubiquilin 2 neuropathological information in post-mortem ALS/FTD human
159 brain tissue, were not primary research articles, or were not published in English were
160 excluded. Seven papers were identified from which neuropathological data for TDP-43,
161 ubiquilin 2, ubiquitin, p62, *C9orf72*-linked DPR proteins, FUS, and SOD1 protein
162 aggregates in the spinal cord and hippocampus were extracted and tabulated.

163 **Patient demographics and hippocampal brain tissue**

164 Formalin-fixed paraffin-embedded (FFPE) post-mortem hippocampal tissue from 6
165 neurologically normal and 30 ALS cases with or without FTD, processed as previously
166 described [45] were obtained from the Neurological Foundation Human Brain Bank at the
167 Centre for Brain Research, Auckland, New Zealand. These included twenty cases with
168 sporadic ALS (one with co-morbid FTD), three with familial ALS of unknown genotype,
169 one with *SOD1*-linked ALS (p.E101G), five with *C9orf72*-linked ALS, and one with
170 ALS+FTD with the *UBQLN2* p.T487I mutation (pedigree ID FALS5 IV:18 in Fig. 1A of
171 [17] and in this report; coded MN17 in Figure 1D of [38] and in this report), giving a total
172 cohort of 41 cases. Note that MN17 was stored in fixative for 7 years before embedding.
173 All non-*SOD1*-linked NZ cases had confirmed pTDP-43 proteinopathy in the motor cortex.
174 FFPE hippocampal tissue was also obtained from: the Victoria Brain Bank from a relative
175 of the *UBQLN2* p.T487I case (p.T487I, ALS+FTD; pedigree ID V:7 in Fig. 1A of [17] and
176 in this report); the London Neurodegenerative Diseases Brain Bank and Brains for
177 Dementia from an unrelated *UBQLN2*-linked case (p.P506S, ALS+FTD:, pedigree ID II.2
178 in Fig. 1B of [15]), and a case with a *UBQLN2* variant of unknown significance (p.S222G,
179 progressive supranuclear palsy; Supplemental_variant_data of [46]), and a *FUS*-linked
180 case (p.P525L, ALS); and from the Northwestern University Feinberg School of Medicine,
181 USA from another unrelated *UBQLN2*-linked case (p.P497H, ALS; pedigree ID V:I of
182 Family #186 in Fig. 1A of [1]). All clinical and neuropathological diagnoses were

183 conducted as described previously [1,15,17,38]. Patient demographic and clinical
184 information is summarised in Supplementary Table 1.

185 **Fluorescent immunohistochemistry and image acquisition**

186 ***Multiplex fluorescent immunohistochemistry***

187 Multiplex (five-label) immunohistochemistry was performed as described previously [47–
188 49]. Briefly, tissue sections were cut with a microtome in the transverse plane at a thickness
189 of 7-10 µm and mounted onto Superfrost Plus slides (Thermo Fisher Scientific). Mounted
190 sections were dried at room temperature for a minimum of 1 week before
191 immunohistochemistry. Slides were heated to 60 °C for 1 h on a hot plate, then dewaxed
192 and rehydrated through a xylene-alcohol-water series: 100% xylene, 2x 30 min; 100%
193 ethanol, 2x 15 min; 95%, 85%, 75% ethanol, 5 min each; water 3x 5 min. Antigens were
194 retrieved through immersion in 10 mM sodium citrate buffer (0.05% Tween 20, pH 6.0) in
195 a pressure cooker (Retriever 2100, Electron Microscopy Sciences) at 120 °C for 20 min
196 and cooled to room temperature for 100 min. Sections were washed 3x 5 min in 1x
197 phosphate-buffered saline (PBS) and wax borders were drawn with an ImmEdge
198 Hydrophobic Barrier PAP pen. Sections were permeabilised in PBS-T (PBS with 0.2%
199 Triton™ X100) for 15 min at 4 °C, followed by 3x 5-min PBS washes. Lipofuscin
200 autofluorescence was quenched using TrueBlack® Lipofuscin quencher (Biotium) 1:20 in
201 70% ethanol for at least 30 seconds followed by three vigorous water washes. Sections
202 were blocked with 10% normal donkey serum (Thermo Fisher Scientific) in PBS for 1 h
203 before 4 °C overnight incubation with primary antibodies targeting ubiquilin 2,
204 phosphorylated TDP-43 (pTDP-43), p62, and *C9orf72*-linked dipeptide repeat proteins
205 polyGA and polyGP (Supplementary Table 2). Following PBS washes, species- and
206 isotype-specific secondary antibodies and Hoechst 33342 nuclear stain (Supplementary
207 Table 3) were applied for 3 h in 1% normal donkey serum at room temperature. After final
208 3x 5-min PBS washes, sections were coverslipped with #1.5 coverslips (Menzel-Gläser)
209 using ProLong™ Gold Antifade Mountant (Thermo Fisher Scientific). All primary
210 antibodies used in this study have been previously validated in human brain tissue
211 [6,38,50,51], and secondary antibodies showed no non-specific binding or signal bleed-

212 through into adjacent channels (Supplementary Fig. 1) or cross-reactivity (Supplementary
213 Fig. 2).
214
215 Multiplex (five-label) images were acquired using a Zeiss Z2 Axioimager with a
216 MetaSystems VSlide slide scanning microscope (20x dry magnification lens, 0.9 NA) with
217 a Colibri 7 solid-state fluorescent light source. Sections were imaged with the same
218 exposure time and gain settings for each staining combination where possible. *UBQLN2*-
219 linked ALS/FTD case V:7-p.T487I showed consistently poor Hoechst immunoreactivity,
220 while *UBQLN2*-linked ALS/FTD case MN17-p.T487I showed poor immunoreactivity
221 overall, likely due to long-term fixation, therefore a longer exposure was used for both
222 cases when imaging. Single filters, as described and validated previously [49], were used
223 to excite fluorophores and detect the following wavelengths: Filter set #1 (LED 385; Em
224 447/60 nm), #3 (LED 475; Em 527/20 nm), #4 (LED 555; Em 580/23 nm), #5 (LED 590;
225 Em 628/32 nm), #6 (LED 630; Em 676/29 nm), and #7 (LED 735; Em 809/81 nm) and
226 visualised with MetaFer software (MetaSystems, v.3.12.1) equipped with a CoolCube 4m
227 TEC (monochrome) sCMOS digital camera. Image tiles were seamlessly stitched using
228 MetaCyte software, and stitched images were extracted using VSViewer software
229 (MetaSystems, v.1.1.106).

230 ***Double-label immunohistochemistry***

231 For super-resolution stimulated emission depleted (STED) microscopy of *C9orf72*-linked
232 ALS case MN28, double-label immunohistochemistry was performed.
233 Immunohistochemistry was performed as above with primary antibody targeting ubiquilin
234 2 and detected by goat anti-mouse IgG_{2a} Alexa Fluor 594, but with primary antibody
235 targeting polyGA detected by goat anti-mouse IgG_1 Biotin (A10519, Thermo Fisher
236 Scientific), followed by 3x 5-min PBS washes, and an additional incubation with Star Red
237 neutravidin (STRED-0121, Abberior) for 1 hour at room temperature. After final 3x 5-min
238 PBS washes, sections were coverslipped with #1.5 coverslips using ProLong™ Glass
239 Antifade Mountant (P36984, Thermo Fisher Scientific).
240

241 STED images were acquired using an Abberior Facility STED microscope (60x
242 UPLXAPO oil immersion lens, 1.42 NA) using ImSpector Lightbox software (Specim,
243 v.16.3.13779). A 561-nm pulsed diode laser was used to excite Alexa Fluor 594, and a
244 640-nm diode laser was used to excite Alexa Fluor 647. For STED imaging, a pulsed 775-
245 nm laser was used for depletion of both fluorophores. After scanning, the images were
246 processed using the PureDenoise plugin [52] for ImageJ (National Institutes of Health,
247 USA v1.53f51).
248
249 Final figures of multiplex and double-label immunohistochemistry were compiled using
250 Adobe Photoshop CC (Adobe Systems Incorporated, v24.4.1). For clarity, multiplex labels
251 are shown in separate panels, either pTDP-43, ubiquilin 2, and p62, or ubiquilin 2, polyGA,
252 and polyGP, with negative labelling not shown.

253 **Relatedness analysis**

254 To further examine the p.T487I mutation in ALS/FTD, genome-wide genotype data from
255 the family of *UBQLN2*-linked ALS+FTD case MN17 (FALS5) and another Australian
256 family with an identical p.T487I mutation (FALS14) were analysed to determine whether
257 they inherited the mutation from a common ancestor (pedigree in Supplementary Fig. 3,
258 sample information in Supplementary Table 4). These two families were previously
259 reported to share a haplotype identical-by-state over the *UBQLN2* locus [17], but genealogy
260 analysis had been unable to link the pedigrees. Three individuals from FALS5 (all affected,
261 pedigree IDs III:8, IV:9, IV:18 (MN17)) and two individuals from FALS14 (pedigree IDs
262 II:1 (unaffected) and III:2 (affected)) underwent SNP genotyping using the Illumina
263 Infinium Global Screening Array v2.0. Identity-by-descent (IBD) analysis was performed
264 using XIBD software [53] with the combined HapMap Phase II and III European (CEU)
265 cohort as a reference dataset. SNPs in high linkage disequilibrium ($r^2 > 0.95$) or SNPs with
266 a low minor allele frequency (MAF < 0.01) were removed from analysis, as well as SNPs
267 with missing genotype calls in two or more samples. 39,002 SNPs remained for analysis
268 and 211 IBD segments greater than 3 cM were identified. The degree of relationship was
269 estimated for each pair of samples using the lengths of inferred IBD segments as in
270 Estimation of Recent Shared Ancestry [54].

271 # Results

272 **Ubiquilin 2 labelling in previous studies failed to discriminate between *UBQLN2*-**
273 **linked and other genotypes of ALS/FTD**

274 Systematic review of the literature describing ubiquilin 2 neuropathology in human
275 ALS/FTD identified 137 results, of which 7 articles met the criteria for full review. The
276 hippocampal neuropathology of ubiquilin 2 with respect to five other ALS/FTD-linked
277 proteins is summarised in Fig. 1. Ubiquilin 2 aggregate deposition in the hippocampal
278 molecular layer was most frequently reported upon, being found in *UBQLN2*-linked and
279 *C9orf72*-linked ALS/FTD, sometimes together with ubiquitin or p62 [6]. Ubiquilin 2
280 aggregate deposition in the granule cell layer of the hippocampal dentate gyrus (GCL) was
281 inconsistent between cases of *UBQLN2*-linked ALS/FTD but was found in all cases of
282 "ALS-dementia" in [1] (all later confirmed to be *C9orf72*-positive) and in a single sporadic
283 ALS/FTD case [15]. Cornu ammonis (CA) ubiquilin 2 pathology had been reported in both
284 *UBQLN2*-linked and *C9orf72*-linked ALS/FTD [1,38,39]. Overall, neither ubiquilin 2
285 staining alone nor in combinations previously tested could distinguish mutant ubiquilin 2
286 aggregation in *UBQLN2*-linked ALS/FTD from wildtype ubiquilin 2 aggregation in other
287 ALS/FTD genotypes.

288 **Ubiquilin 2 and other pathology in ALS/FTD of various genotypes**

289 ***Control and familial ALS cases had no hippocampal ubiquilin 2 aggregates but certain***
290 ***cases had sparse p62-only aggregates***

291 Five of the six non-neurodegenerative disease control cases included in this study showed
292 no deposition of ubiquilin 2, pTDP-43, p62, or DPR protein aggregates in any region of
293 the hippocampus (not shown). The remaining control case (H230) showed sparse p62
294 aggregates in the GCL and CA pyramidal cell layer (CA – pyr) (Fig. $1A_{1,2}$).
295
296 All five familial ALS cases also showed sparse p62 aggregates in the GCL and CA – pyr
297 regions; three cases were of unknown genotype, represented by case MN14 (Fig. $1B_{1,2}$),
298 one harboured a *SOD1* p.E101G mutation (Fig. $1C_{1,2}$), and one harboured a *FUS* p.P525L

299 mutation (Fig. 1D$_{1,2}$). No other pathology was observed in familial cases in hippocampal
300 regions.

301 ***Sporadic ALS cases had no hippocampal ubiquilin 2 aggregates but certain cases had***
302 ***pTDP-43-p62 aggregates***

303 None of the 20 sporadic ALS cases (one with co-morbid FTD) showed hippocampal
304 ubiquilin 2 or DPR aggregates (not shown). Fourteen cases (70%) were devoid of either
305 ubiquilin 2 or pTDP-43 in the GCL, ML, CA-pyr, and CA – lm/rad layers (not shown),
306 however 4 cases (20%) had compact p62-positive NCIs in the GCL and CA – pyr regions
307 that were negative for all other markers (Supplementary Fig. 4). Six cases (30%; including
308 representative cases MN15 with ALS+FTD, and MN30 with ALS) had compact or net-like
309 perinuclear pTDP-43-positive neuronal cytoplasmic inclusions (NCIs) in the GCL and CA
310 – pyr regions ranging in density from sparse to frequent, suggestive of stage 4 pTDP-43
311 proteinopathy [55]. These pTDP-43 aggregates were almost always p62-positive and
312 ubiquilin 2-negative (Fig. 2E$_{1,2}$ and F$_{1,2}$, white arrows), with the exception of 1-2
313 perinuclear aggregates that were not p62-labelled (Fig. 2F$_1$, yellow arrow).

314 ***C9orf72 cases had molecular layer ubiquilin 2-only aggregates, granule cell layer***
315 ***ubiquilin 2-DPR-p62 aggregates, and one case had granule cell layer ubiquilin 2-DPR-***
316 ***pTDP-43-p62 aggregates***

317 Four of the five *C9orf72*-linked ALS cases showed identical hippocampal pathology
318 (represented by case MN18), while the fifth case (MN28) differed only by having pTDP-
319 43 aggregates in the GCL and CA – pyr, described below.
320

321 All five cases shared a signature of numerous ubiquilin 2 aggregates in the ML, GCL and
322 CA – l-m/rad regions. In the ML and CA – l-m/rad, ubiquilin 2 aggregates were punctate
323 or skein-like, dendritic, and very rarely co-localised with p62 (Fig. 3A$_{1,2}$ and B$_{1,2}$, green
324 arrowheads) and never with DPR proteins (Fig. 3C$_{1,2}$ and D$_{1,2}$, green arrowheads). In the
325 CA – pyr, aggregates did not contain ubiquilin 2 (Fig. 3A$_3$-D$_3$) but were positive for p62
326 (Fig. 3A$_3$, B$_3$, pink arrows), polyGA, and polyGP (Fig 3C$_3$, D$_3$, orange arrows and insets),
327 with pTDP-43 in case MN28 also seen rarely (Fig. 3B$_3$, yellow arrow).
328

329

330 In the GCL, ubiquilin 2 aggregates were perinuclear NCIs that were negative for pTDP-43
331 except rare aggregates in case MN28 (Fig. $3B_4$, yellow arrow), but always positive for p62
332 (Fig. $3A_1$, B_1, white arrows and yellow arrow) and poly(glycine-arginine) (polyGA), but
333 rarely polyGP (Fig $3C_1$, D_1, yellow arrows). Ubiquilin 2 aggregates positive for pTDP-43
334 were rare (1-2 GCL cells per section of MN28) and comprised a pTDP-43 'shell'
335 surrounding polyGA either with polyGP (Supplementary Fig. 5A, white arrow) or without
336 polyGP (Supplementary Fig. 5A, purple arrow). This supports a previous report that
337 ubiquilin 2 in *C9orf72*-linked cases rarely co-localises with GCL pTDP-43, doing so only
338 when DPR proteins are present in the aggregate [56]. Therefore, wildtype ubiquilin 2
339 aggregation may be 'seeded' in the GCL by polyGA rather than by pTDP-43.
340

341 ***UBQLN2 cases show molecular layer ubiquilin 2-p62 aggregates and certain cases had***
342 ***granule cell layer pTDP-43 aggregates***

343 All four *UBQLN2*-linked ALS/FTD cases showed signature ubiquilin 2-positive but pTDP-
344 43-negative punctate aggregates in the hippocampal ML and CA – lm/rad regions, albeit
345 at variable loads (Fig. $4A_{2,3}$, $B_{2,3}$, $C_{2,3}$, $D_{2,3}$, white arrows). In the ML, ubiquilin 2
346 aggregates were punctate and appeared to be localised to the dendritic spines of the granule
347 cells, as reported in *UBQLN2*-linked ALS/FTD and mutant *UBQLN2* rodent models [1,57].
348 In contrast to *C9orf72*-linked cases, these ML ubiquilin 2 aggregates almost always co-
349 localised with p62. The PSP case with a *UBQLN2* p.S222G variant of unknown
350 significance did not share this signature of ubiquilin 2- and p62-positive aggregates in the
351 ML and CA – lm/rad, instead having p62-only aggregates in the CA – lm/rad (Fig. $4E_{2,3}$,
352 pink arrowheads).
353

354 Confocal microscopy of the ML and CA – lm/rad regions confirmed that the p62-positive
355 mutant ubiquilin 2 aggregates in *UBQLN2*-linked ALS/FTD cases (Supplementary Fig.
356 5A, representative p.P506S case shown) differed from wildtype ubiquilin 2 aggregates in
357 those regions in *C9orf72*-linked ALS, which were predominantly p62 negative
358 (Supplementary Fig. 5B, representative case MN28). Further, while mutant ubiquilin 2 in

359 *UBQLN2*-linked cases formed small compact aggregates (Supplementary Fig. 6A)
360 wildtype ubiquilin 2 in *C9orf72*-linked cases formed small compact aggregates and wispy
361 skein-like structures (Supplementary Fig. 6B). Therefore, mutant but not wildtype
362 ubiquilin 2 in the hippocampal ML and CA – lm/rad regions may promote or scaffold the
363 co-aggregation of p62, and there may be structural differences between mutant and
364 wildtype.
365
366 In the GCL, two of the four *UBQLN2*-linked ALS/FTD cases were devoid of pTDP-43,
367 ubiquilin 2, and p62 aggregates, consistent with previous findings [1,38] (case P497H, Fig.
368 4A$_1$; and MN17 – T487I, Fig. 4B$_1$). In contrast, case V:7 – T487I showed very sparse
369 pTDP-43 cytoplasmic aggregates in the GCL that were negative for ubiquilin 2 but weakly
370 positive for p62 (Fig. 4C$_1$, white hollow arrowhead). Consistent with Gkazi and colleagues
371 [15] and with the known spectrum of pTDP-43 loads in the GCL in ALS/FTD [55], the
372 *UBQLN2* p.P506S case had abundant p62-positive pTDP-43 cytoplasmic aggregates in the
373 GCL, that either co-localised with ubiquilin 2 (Fig. 4D$_1$, white filled arrowheads) or were
374 independent of ubiquilin 2 (Fig. 4D$_1$, white hollow arrowheads). Mutant ubiquilin 2
375 aggregation in the GCL was therefore likely scaffolded or 'seeded' by pTDP-43 when
376 present. The *UBQLN2* p.S222G PSP case showed sparse p62-only aggregates in the GCL
377 that were not seen in *UBQLN2*-linked ALS/FTD cases (Fig. 4E$_1$, pink arrowheads).
378
379 *UBQLN2*-linked ALS/FTD case P506S also had sparse pTDP-43 aggregates in the CA –
380 pyr cells, which were positive for both ubiquilin 2 and p62 (Fig. 4D$_3$, white filled
381 arrowhead). All *UBQLN2* variant and mutation cases were negative for DPRs (not shown).

382 **Combined neuropathological signatures discriminate between *UBQLN2*-linked,**
383 ***C9orf72*-linked, sporadic, and familial cases**

384 Integration of all neuropathological findings (Fig. 5) revealed a characteristic hippocampal
385 neuropathological signature for *UBQLN2*-linked ALS/FTD, that was distinct from that in
386 other forms of ALS/FTD. Sporadic ALS cases were wholly devoid of hippocampal
387 ubiquilin 2 or DPR protein pathology, with a minority of cases showing pTDP-43
388 aggregates in the granule cells that were ubiquilin 2 negative. Thus, wildtype ubiquilin 2

389 is not seeded/ scaffolded to aggregate by pTDP-43 aggregation. *C9orf72*-linked cases
390 showed ML ubiquilin 2 aggregates that were wispy or punctate and predominantly p62
391 negative, while *UBQLN2*-linked cases showed ML ubiquilin 2 aggregates that were
392 punctate and predominantly p62 positive. Mutant ubiquilin 2 aggregates thus promote the
393 co-aggregation of p62, and this may relate to their conformational differences. Overall,
394 mutant ubiquilin 2 causes unique neuropathology that is shared by p.P506S, p.P497H, and
395 p.T487I ubiquilin 2 (Fig. 6). The absence of this signature in a case harbouring a p.S222G
396 variant manifesting with PSP suggests this neuropathology can be used to discriminate
397 pathological ALS/FTD-causing *UBQLN2* mutations.
398
399 Ubiquilin 2 hippocampal pathology was present in both *UBQLN2*-linked ALS/FTD and
400 *C9orf72*-linked ALS, but these genotypes could be discriminated when ubiquilin 2 was co-
401 labelled with pTDP-43, DPR proteins, or p62. *C9orf72*-linked cases always showed GCL
402 ubiquilin 2 that co-localised with DPR aggregates, but rarely pTDP-43. This supports the
403 lack of seeding of wildtype ubiquilin 2 aggregation by pTDP-43 but suggests that wildtype
404 ubiquilin 2 can be seeded by polyGA. In contrast, *UBQLN2*-linked cases showed GCL
405 ubiquilin 2 if co-localised pTDP-43 was present. Therefore, mutant ubiquilin 2 is more
406 aggregation-prone than wildtype, being seeded by pTDP-43.

407 ***UBQLN2* p.T487I mutation in ALS/FTD families FALS5 and FALS14 was inherited**
408 **from a common ancestor**

409 Since the initial report by Williams et al. [17] of an identical *UBQLN2* p.T487I mutation
410 in ALS families FALS5 and FALS14, we report here that cases MN17 (IV:18) and V:7
411 from family FALS5 developed ALS+FTD, indicating that FTD is part of the clinical
412 phenotype in that family. To further examine relatedness between the families and confirm
413 that the *UBQLN2* p.T487I mutation arose in a common founder, we performed identity-
414 by-descent (IBD) analysis. IBD segments were identified over the *UBQLN2* locus between
415 all four affected individuals from both families (Table 1), while there were no IBD
416 segments inferred over *UBQLN2* between the affected individuals from FALS5 and the
417 unaffected individual from FALS14 who did not carry the *UBQLN2* p.T487I mutation. The
418 interval shared by all four affected individuals spanned rs952836 to rs6423133 and is 68

419 cM in length. This confirms a founder effect of *UBQLN2* p.T487I in FALS5 and FALS14.
420 The genotyped individuals across these families are estimated to be 4th- to 5th-degree
421 relatives (1st cousins once removed - 2nd cousins) (Table 2), now confirming segregation
422 of the *UBQLN2* p.T487I mutation in 17 individuals from the proposed combined Australia-
423 New Zealand pedigree and providing further strong genetic evidence, in addition to the
424 neuropathological evidence, that *UBQLN2* p.T487I is pathogenic for ALS/FTD.

425 ## Discussion

426 ALS shows considerable clinical, pathological, and genetic heterogeneity [58–60]. While
427 TDP-43 proteinopathy is seen in 97% of cases [40,43,61], ALS/FTD-causing genetic
428 mutations can cause deposition of the encoded mutant protein leading to additional
429 pathological aggregate signatures. We previously exploited this to infer *C9orf72* repeat
430 expansion genotypes [62,63] through neuropathological screening of our New Zealand
431 ALS cases [38]. Mutant *SOD1* [64,65], *FUS* [44], and certain other genotypes [66,67] can
432 also be inferred from neuropathology. However, for many ALS/FTD genes — particularly
433 those such as *TARDBP*, *SQSTM1*, and *UBQLN2* that encode proteins already within the
434 hallmark TDP-43 inclusions — no completely discriminating neuropathology has been
435 reported [42,66,68–72]. This has hampered the validation of pathogenicity of novel
436 variants in these genes, in turn obscuring understanding of protein domains and molecular
437 processes important to ALS/FTD pathogenesis. However, we report here a unique
438 neuropathological signature for mutant ubiquilin 2 in the hippocampus that discriminates
439 *UBQLN2*-linked ALS/FTD cases from all others tested.

440 **pTDP-43 in *UBQLN2*-linked cases: An independent pathology**

441 Before discussing the unique pattern of hippocampal ubiquilin 2 pathology shared by
442 *UBQLN2*-linked cases, it must first be noted that pTDP-43 deposition was variable. Two
443 of the four *UBQLN2*-linked cases were devoid of GCL pTDP-43 aggregates (p.P497H
444 (ALS) and MN17-p.T487I (ALS+FTD)), one case had very sparse GCL pTDP-43
445 aggregates that were ubiquilin 2-negative (V:7-p.T487I (ALS+FTD)), and one case
446 showed frequent GCL pTDP-43 aggregates that were mostly ubiquilin 2-positive (p.P506S
447 (ALS+FTD)). Although pTDP-43 aggregates are nearly ubiquitous in the ALS spinal cord
448 and motor cortex, only in ~15-30% of ALS cases are they found in the hippocampus
449 [55,73]. Our findings suggest that variable regional pTDP-43 deposition occurs in the
450 context of *UBQLN2*-linked ALS/FTD just as it does in sporadic and *C9orf72*-linked
451 ALS/FTD.

452 **Wildtype ubiquilin 2 pathology in *C9orf72*-linked cases**

453 Hippocampal ubiquilin 2 deposition is a known and striking feature of *C9orf72*-linked
454 ALS/FTD [39]. In our *C9orf72*-linked ALS cases, large stellate GCL ubiquilin 2 was found
455 to preferentially co-localise with the aggregation-prone polyGA DPR protein compared to
456 polyGP. Furthermore, polyGP aggregates were very rarely independent of polyGA. These
457 findings support the emerging consensus that polyGA aggregates 'seed' polyGP protein
458 aggregation [74–76]. Similar observations were made by Mackenzie and colleagues [56]
459 of aggregates with a core of polyGA surrounded by an aggregated TDP-43 shell; a finding
460 recapitulated here and supported by *in vitro* work showing polyGA aggregation preceding
461 TDP-43 accumulation [77]. The ability of DPR proteins to seed ubiquilin 2 however,
462 appears more complex. We previously showed ubiquilin 2 at the core of polyGP-positive
463 aggregates, but we did not co-label for polyGA [38]. STED imaging in the current study
464 shows that ubiquilin 2 may either surround polyGA or be enmeshed with it, suggesting that
465 in *C9orf72*-linked ALS pathogenesis, the interaction between aggregating polyGA and
466 ubiquilin 2 may be an early event.
467
468 In contrast to ubiquilin 2 co-aggregation with large stellate DPR proteins in the GCL, small
469 neuritic ubiquilin 2 aggregates in *C9orf72*-linked cases punctuated the ML, and CA –
470 lm/rad regions seemingly independent of a nucleating protein. The neurites in which these
471 small aggregates are found likely derive from the granule or pyramidal cells, respectively
472 [78,79], so DPR protein inclusions in the somata may promote the aggregation of ubiquilin
473 2 in the dendrites of the same cell. DPR aggregates can sequester proteasome components
474 [80–82], and loss of C9orf72 protein function in cells expressing the DPR-encoding variant
475 2 [83] can impair autophagy [84–89], which may underpin wildtype ubiquilin 2
476 aggregation in the ML, and CA – lm/rad layers in *C9orf72*-linked cases.

477 **Mutant ubiquilin 2 pathology in *UBQLN2*-linked cases: A neuropathological**
478 **signature**

479 Even in its wildtype state, ubiquilin 2 intrinsically self-assembles [3] but there is now ample
480 biophysical evidence demonstrating that mutations to ubiquilin 2 confer an increased
481 propensity to oligomerise and undergo aberrant LLPS, forming insoluble aggregates within

482 the cell [8,9,12,90–92]. Here we confirm that mutant ubiquilin 2 in the human hippocampal
483 ML (granule cell dendrites) is aggregated under less permissive conditions than wildtype
484 ubiquilin 2, appearing to require no aggregated protein scaffold, or protein aggregation
485 event in the GCL (granule cell soma).
486
487 Our study additionally found that p62 labelling was required, while pTDP-43 labelling was
488 dispensable, to confirm cases as being *UBQLN2*-linked. P62 co-localises with pTDP-43
489 aggregates and DPR proteins in ALS/FTD [62,93,94], or with hyperphosphorylated tau in
490 a range of tauopathies [95–97], or with mutant α-synuclein in synucleinopathies [97,98].
491 Given this promiscuity for substrates, discrimination between mutant and wildtype
492 ubiquilin 2 by p62 suggests that there are unique structural or biochemical features of
493 mutant ubiquilin 2 aggregates. This leads to the intriguing possibility that mutant ubiquilin
494 2 would be selectively druggable.
495
496 In addition to mechanistic insights, the mutant ubiquilin 2 neuropathological signature we
497 describe will enable classification of *UBQLN2* variants of uncertain significance, clarifying
498 the implications of a positive genetic result in a patient. Currently, only four missense
499 mutations in *UBQLN2* are designated by ClinVar as pathogenic or likely pathogenic
500 (resulting in p.M392V, p.Q425R, p.P497H, p.P497S, p.P506T,
501 https://www.ncbi.nlm.nih.gov/clinvar/, accessed July 11 2023 [99]). However, 62 other
502 *UBQLN2* missense changes listed in ClinVar are classified as benign or of uncertain
503 significance, including c.1516C>T resulting in p.P506S. Indeed, neither *UBQLN2* p.T487I
504 nor p.S222G are even listed in ClinVar, leaving individual diagnostics labs to perform
505 classification for patient reporting. We now confirm that two ALS/FTD cases with p.T487I,
506 which segregates with disease in a large kindred and shows early onset in males consistent
507 with X-linked disease, shared our newly identified mutant ubiquilin 2 neuropathological
508 signature, supporting its classification as pathogenic. Conversely, a male PSP case with
509 p.S222G who lived to 93 y did not share this signature, suggesting this variant is benign.
510 We encourage uptake of this hippocampal ubiquilin 2 neuropathology signature, by other
511 labs or in collaboration with the authors hereof, as a tool to explore *UBQLN2* variant
512 pathogenicity.

513 ## Conclusion

514 Ubiquilin 2 aggregates were seen in the hippocampus of ALS/FTD cases across a range of
515 genotypes. Wildtype ubiquilin 2 *in vitro* is known to be aggregation-prone; in human brain
516 it co-aggregated with polyGA, but not pTDP-43 and with little co-aggregation of p62.
517 Mutant ubiquilin 2 *in vitro* is known to be more aggregation-prone than wildtype; in brain
518 it was either co-aggregated with pTDP-43 or aggregated independently of a known scaffold
519 and appeared to promote the co-aggregation of p62. This hippocampal ubiquilin 2
520 neuropathology signature demonstrates that ubiquilin 2 aggregation is likely to play a
521 mechanistic role in *C9orf72*-linked and *UBQLN2*-linked ALS/FTD and provides a
522 definitive framework for exploring the biological implications of *UBQLN2* genetic
523 variation.

524 **List of abbreviations**

525	ALS	Amyotrophic lateral sclerosis
526	bvFTD	Behavioural variant FTD
527	CA-lm/rad	Cornu ammonis lacunosum-molecular and radiatum layers
528	CA-pyr	Cornu ammonis pyramidal layer
529	C9orf72	Chromosome 9 open reading frame 72
530	DPR	Dipeptide repeat
531	FFPE	Formalin-fixed paraffin-embedded
532	FTD	Frontotemporal dementia
533	GCL	Granule cell layer
534	IBD	Identity by descent
535	LLPS	Liquid-liquid phase separation
536	ML	Molecular layer
537	NCI	Neuronal cytoplasmic inclusions
538	PBS	Phosphate-buffered saline
539	PolyGA	Poly(glycine-arginine)
540	PolyGP	Poly(glycine-proline)
541	pTDP-43	Phosphorylated TDP-43
542	SOD1	Superoxide dismutase
543	STED	Stimulated emission depletion
544	SQSTM1	Sequestosome 1
545	TDP-43	Transactive response DNA binding protein 43 kDa

Disclosures and declarations

Data transparency

The datasets used and/or analysed during the current study are available from the corresponding author on reasonable request.

Compliance with ethical standards

Conflicts of interest

The authors declare that they have no conflicts of interest.

Research involving human participants

All protocols were approved by the University of Auckland Human Participants Ethics Committee (New Zealand) and carried out as per approved guidelines. This study was also approved by the Human Research Ethics Committee of Macquarie University (520211013428875).

Informed consent

Informed donor consent and ethical approvals were obtained at each site as described previously [1,15,17,38].

563 **References**

564 1. Deng H-XX, Chen W, Hong S-TT, Boycott KM, Gorrie GH, Siddique N, et al.
565 Mutations in UBQLN2 cause dominant X-linked juvenile and adult-onset ALS
566 and ALS/dementia. Nature. 2011;477(7363):211–5. doi:10.1038/nature10353
567 2. Marín I. The ubiquilin gene family: Evolutionary patterns and functional
568 insights. BMC Evol Biol. 2014;14(1):1–22. 10.1186/1471-2148-14-63
569 3. Hjerpe R, Bett JS, Keuss MJ, Solovyova A, McWilliams TG, Johnson C, et al.
570 UBQLN2 Mediates Autophagy-Independent Protein Aggregate Clearance by
571 the Proteasome. Cell. 2016;166(4):935–49. 10.1016/j.cell.2016.07.001
572 4. Itakura E, Zavodszky E, Shao S, Wohlever ML, Keenan RJ, Hegde RS.
573 Ubiquilins Chaperone and Triage Mitochondrial Membrane Proteins for
574 Degradation. Mol Cell. 2016;63(1):21–33. 10.1016/j.molcel.2016.05.020
575 5. Protter DSW, Parker R. Principles and Properties of Stress Granules. Trends
576 Cell Biol. 2016;26(9):668–79. 10.1016/j.tcb.2016.05.004
577 6. Wu JJ, Cai A, Greenslade JE, Higgins NR, Fan C, Le NTT, et al. ALS/FTD
578 mutations in UBQLN2 impede autophagy by reducing autophagosome
579 acidification through loss of function. Proceedings of the National Academy of
580 Sciences. 2020;2(Line 356):201917371.
581 7. Alexander EJ, Niaki AG, Zhang T, Sarkar J, Liu Y, Nirujogi RS, et al.
582 Ubiquilin 2 modulates ALS/FTD-linked FUS–RNA complex dynamics and
583 stress granule formation. Proc Natl Acad Sci U S A. 2018;115(49):E11485–94.
584 8. Dao TP, Kolaitis RM, Kim HJ, O'Donovan K, Martyniak B, Colicino E, et al.
585 Ubiquitin Modulates Liquid-Liquid Phase Separation of UBQLN2 via
586 Disruption of Multivalent Interactions. Mol Cell. 2018;69(6):965-978.e6.
587 9. Sharkey LM, Safren N, Pithadia AS, Gerson JE, Dulchavsky M, Fischer S, et
588 al. Mutant UBQLN2 promotes toxicity by modulating intrinsic self-assembly.
589 Proceedings of the National Academy of Sciences. 2018 Oct
590 30;115(44):E10495–504. 10.1073/pnas.1810522115
591 10. Subudhi I, Shorter J. Ubiquilin 2: Shuttling Clients Out of Phase? Mol Cell.
592 2018;69(6):919–21. 10.1016/j.molcel.2018.02.030

593 11. Chang L, Monteiro MJ. Defective proteasome delivery of polyubiquitinated
594 proteins by ubiquilin-2 proteins containing ALS mutations. PLoS One.
595 2015;10(6):1–15. 10.1371/journal.pone.0130162
596 12. Dao TP, Martyniak B, Canning AJ, Lei Y, Colicino EG, Cosgrove MS, et al.
597 ALS-Linked Mutations Affect UBQLN2 Oligomerization and Phase
598 Separation in a Position- and Amino Acid-Dependent Manner. Structure.
599 2019;27(6):937-951.e5.
600 13. Gilpin KM, Chang L, Monteiro MJ. ALS-linked mutations in ubiquilin-2 or
601 hnRNPA1 reduce interaction between ubiquilin-2 and hnRNPA1. Hum Mol
602 Genet. 2015 May 1;24(9):2565–77. 10.1093/hmg/ddv020
603 14. Higgins N, Lin B, Monteiro MJ. Lou Gehrig's Disease (ALS): UBQLN2
604 Mutations Strike Out of Phase. Structure. 2019;27(6):879–81.
605 10.1016/j.str.2019.05.006
606 15. Gkazi SA, Troakes C, Topp S, Miller JW, Vance CA, Sreedharan J, et al.
607 Striking phenotypic variation in a family with the P506S UBQLN2 mutation
608 including amyotrophic lateral sclerosis, spastic paraplegia, and frontotemporal
609 dementia. Neurobiol Aging. 2019;73:229.e5-229.e9.
610 10.1016/j.neurobiolaging.2018.08.015
611 16. McCann EP, Williams KL, Fifita JA, Tarr IS, O'Connor J, Rowe DB, et al. The
612 genotype-phenotype landscape of familial amyotrophic lateral sclerosis in
613 Australia. Clin Genet. 2017 Sep;92(3):259–66. 10.1111/cge.12973
614 17. Williams KL, Warraich ST, Yang S, Solski JA, Fernando R, Rouleau GA, et
615 al. UBQLN2/ubiquilin 2 mutation and pathology in familial amyotrophic
616 lateral sclerosis. Neurobiol Aging. 2012;33(10):2527.e3-2527.e10.
617 10.1016/j.neurobiolaging.2012.05.008
618 18. Chen J, Liu X, Xu Y, Fan D. Association between rare UBQLN2 variants and
619 amyotrophic lateral sclerosis in Chinese population. National Medical Journal
620 of China. 2021;101(12):846–50.
621 19. Kim HJ, Kwon MJ, Choi WJ, Oh KW, Oh S il, Ki CS, et al. Mutations in
622 UBQLN2 and SIGMAR1 genes are rare in Korean patients with amyotrophic

623 lateral sclerosis. Neurobiol Aging. 2014;35(8):1957.e7-1957.e8.
624 10.1016/j.neurobiolaging.2014.03.001
625 20. Baglivo M, Manara E, Capodicasa N, Maltese PE, Stuppia L, Michelini S, et
626 al. Early-onset of Frontotemporal Dementia and Amyotrophic Lateral Sclerosis
627 in an Albanian Patient with a c.1319C>T Variant in the UBQLN2 Gene. Open
628 Med J. 2020;7(1):25–31. 10.2174/1874220302007010025
629 21. Daoud H, Suhail H, Szuto A, Camu W, Salachas F, Meininger V, et al.
630 UBQLN2 mutations are rare in French and French-Canadian amyotrophic
631 lateral sclerosis. Neurobiol Aging. 2012;33(9):2230.e1-2230.e5.
632 10.1016/j.neurobiolaging.2012.03.015
633 22. Dillen L, van Langenhove T, Engelborghs S, Vandenbulcke M, Sarafov S,
634 Tournev I, et al. Explorative genetic study of UBQLN2 and PFN1 in an
635 extended Flanders-Belgian cohort of frontotemporal lobar degeneration
636 patients. Neurobiol Aging. 2013;34(6):1711.e1-1711.e5.
637 23. Fahed AC, McDonough B, Gouvion CM, Newell KL, Dure LS, Bebin M, et al.
638 UBQLN2 mutation causing heterogeneous X-linked dominant
639 neurodegeneration. Ann Neurol. 2014;75(5):793–8.
640 24. Gellera C, Tiloca C, del Bo R, Corrado L, Pensato V, Agostini J, et al. Ubiquilin
641 2 mutations in Italian patients with amyotrophic lateral sclerosis and
642 frontotemporal dementia. J Neurol Neurosurg Psychiatry. 2013;84(2):183–7.
643 10.1136/jnnp-2012-303433
644 25. Huang X, Shen S, Fan D. No evidence for pathogenic role of UBQLN2
645 mutations in sporadic amyotrophic lateral sclerosis in the mainland Chinese
646 population. Le W, editor. PLoS One. 2017;12(1):1–5.
647 10.1371/journal.pone.0170943
648 26. Lattante S, le Ber I, Camuzat A, Pariente J, Brice A, Kabashi E. Screening
649 UBQLN-2 in French frontotemporal lobar degeneration and frontotemporal
650 lobar degeneration-amyotrophic lateral sclerosis patients. Neurobiol Aging.
651 2013;34(8):2078.e5-2078.e6.
652 27. Luukkainen L, Helisalmi S, Kytövuori L, Ahmasalo R, Solje E, Haapasalo A,
653 et al. Mutation Analysis of the Genes Linked to Early Onset Alzheimer's

654 Disease and Frontotemporal Lobar Degeneration. Journal of Alzheimer's
655 Disease. 2019 Jun 4;69(3):775–82. 10.3233/JAD-181256
656 28. McLaughlin RL, Kenna KP, Vajda A, Byrne S, Bradley DG, Hardiman O, et
657 al. UBQLN2 mutations are not a frequent cause of amyotrophic lateral sclerosis
658 in ireland. Neurobiol Aging. 2014;35(1):267.e9-267.e11.
659 10.1016/j.neurobiolaging.2013.07.023
660 29. Millecamps S, Corcia P, Cazeneuve C, Boillée S, Seilhean D, Danel-Brunaud
661 V, et al. Mutations in UBQLN2 are rare in French amyotrophic lateral sclerosis.
662 Neurobiol Aging. 2012;33(4):839.e1-839.e3.
663 10.1016/j.neurobiolaging.2011.11.010
664 30. Morgan S, Shatunov A, Sproviero W, Jones AR, Shoai M, Hughes D, et al. A
665 comprehensive analysis of rare genetic variation in amyotrophic lateral
666 sclerosis in the UK. Brain. 2017 Jun 1;140(6):1611–8. 10.1093/brain/awx082
667 31. Özoğuz A, Uyan Ö, Birdal G, Iskender C, Kartal E, Lahut S, et al. The distinct
668 genetic pattern of ALS in Turkey and novel mutations. Neurobiol Aging.
669 2015;36(4):1764.e9-1764.e18. 10.1016/j.neurobiolaging.2014.12.032
670 32. Synofzik M, Maetzler W, Grehl T, Prudlo J, vom Hagen JM, Haack T, et al.
671 Screening in ALS and FTD patients reveals 3 novel UBQLN2 mutations
672 outside the PXX domain and a pure FTD phenotype. Neurobiol Aging.
673 2012;33(12):2949.e13-2949.e17. 10.1016/j.neurobiolaging.2012.07.002
674 33. Teyssou E, Chartier L, Amador M-D-M, Lam R, Lautrette G, Nicol M, et al.
675 Novel UBQLN2 mutations linked to amyotrophic lateral sclerosis and atypical
676 hereditary spastic paraplegia phenotype through defective HSP70-mediated
677 proteolysis. Neurobiol Aging. 2017 Oct;58(March):239.e11-239.e20.
678 10.1016/j.neurobiolaging.2017.06.018
679 34. Tripolszki K, Gampawar P, Schmidt H, Nagy ZF, Nagy D, Klivényi P, et al.
680 Comprehensive Genetic Analysis of a Hungarian Amyotrophic Lateral
681 Sclerosis Cohort. Front Genet. 2019 Aug 16;10(JUL).
682 10.3389/fgene.2019.00732
683 35. Ugwu F, Rollinson S, Harris J, Gerhard A, Richardson A, Jones M, et al. A
684 UBQLN2 variant of unknown significance in frontotemporal lobar

685 degeneration. Neurobiol Aging. 2015 Jan;36(1):546.e15-546.e16.
686 10.1016/j.neurobiolaging.2014.08.002
687 36. Vengoechea J, David MP, Yaghi SR, Carpenter L, Rudnicki SA. Clinical
688 variability and female penetrance in X-linked familial FTD/ALS caused by a
689 P506S mutation in UBQLN2. Amyotroph Lateral Scler Frontotemporal
690 Degener. 2013 Dec 14;14(7–8):615–9. 10.3109/21678421.2013.824001
691 37. Vildan C, Sule D, Turker B, Hilmi U, Sibel KB. Genetic alterations of C9orf72,
692 SOD1, TARDBP, FUS, and UBQLN2 genes in patients with Amyotrophic
693 Lateral Sclerosis. Cogent Med. 2019;6(1):1–10.
694 10.1080/2331205x.2019.1582400
695 38. Scotter EL, Smyth L, Bailey JWT, Wong C-H, de Majo M, Vance CA, et al.
696 C9ORF72 and UBQLN2 mutations are causes of amyotrophic lateral sclerosis
697 in New Zealand: a genetic and pathologic study using banked human brain
698 tissue. Neurobiol Aging. 2017 Jan;49:214.e1-214.e5.
699 10.1016/j.neurobiolaging.2016.06.019
700 39. Brettschneider J, Van Deerlin VM, Robinson JL, Kwong L, Lee EB, Ali YO,
701 et al. Pattern of ubiquilin pathology in ALS and FTLD indicates presence of
702 C9ORF72 hexanucleotide expansion. Acta Neuropathol. 2012 Jun
703 18;123(6):825–39. 10.1007/s00401-012-0970-z
704 40. Arai T, Hasegawa M, Akiyama H, Ikeda K, Nonaka T, Mori H, et al. TDP-43
705 is a component of ubiquitin-positive tau-negative inclusions in frontotemporal
706 lobar degeneration and amyotrophic lateral sclerosis. Biochem Biophys Res
707 Commun. 2006;351(3):602–11. 10.1016/j.bbrc.2006.10.093
708 41. Kwiatkowski TJ, Bosco DA, LeClerc AL, Tamrazian E, Vanderburg CR, Russ
709 C, et al. Mutations in the FUS/TLS gene on chromosome 16 cause familial
710 amyotrophic lateral sclerosis. Science (1979). 2009;323(5918):1205–8.
711 10.1126/science.1166066
712 42. Maruyama H, Morino H, Ito H, Izumi Y, Kato H, Watanabe Y, et al. Mutations
713 of optineurin in amyotrophic lateral sclerosis. Nature. 2010;465(7295):223–6.
714 43. Neumann M, Sampathu DM, Kwong LK, Truax AC, Micsenyi MC, Chou TT,
715 et al. Ubiquitinated TDP-43 in Frontotemporal Lobar Degeneration and

716 Amyotrophic Lateral Sclerosis. Science (1979). 2006 Oct 6;314(5796):130–3.
717 10.1126/science.1134108
718 44. Vance C, Rogelj B, Hortobagyi T, de Vos KJ, Nishimura AL, Sreedharan J, et
719 al. Mutations in FUS, an RNA Processing Protein, Cause Familial
720 Amyotrophic Lateral Sclerosis Type 6. Science (1979). 2009 Feb
721 27;323(5918):1208–11. 10.1126/science.1165942
722 45. Waldvogel HJ, Bullock JY, Synek BJ, Curtis MA, van Roon-Mom WMC,
723 Faull RLM. The collection and processing of human brain tissue for research.
724 Cell Tissue Bank. 2008 Sep 21;9(3):169–79. 10.1007/s10561-008-9068-1
725 46. Keogh MJ, Wei W, Wilson I, Coxhead J, Ryan S, Rollinson S, et al. Genetic
726 compendium of 1511 human brains available through the UK Medical
727 Research Council Brain Banks Network Resource. Genome Res.
728 2017;27(1):165–73.
729 47. Murray HC, Johson K, Sedlock A, Highet B, Dieriks BV, Anekal PV, et al.
730 Lamina-specific immunohistochemical signatures in the olfactory bulb of
731 healthy, Alzheimer's and Parkinson's disease patients. Commun Biol.
732 2021;5(1):88. 10.1038/s42003-022-03032-5
733 48. Waldvogel HJ, Curtis MA, Baer K, Rees MI, Faull RLM.
734 Immunohistochemical staining of post-mortem adult human brain sections. Nat
735 Protoc. 2007;1(6):2719–32. 10.1038/nprot.2006.354
736 49. Maric D, Jahanipour J, Li XR, Singh A, Mobiny A, Van Nguyen H, et al.
737 Whole-brain tissue mapping toolkit using large-scale highly multiplexed
738 immunofluorescence imaging and deep neural networks. Nat Commun.
739 2021;12(1):1550. 10.1038/s41467-021-21735-x
740 50. Liu F, Morderer D, Wren MC, Vettleson-Trutza SA, Wang Y, Rabichow BE,
741 et al. Proximity proteomics of C9orf72 dipeptide repeat proteins identifies
742 molecular chaperones as modifiers of poly-GA aggregation. Acta Neuropathol
743 Commun. 2022;10(1):1–18. 10.1186/s40478-022-01322-x
744 51. Neumann M, Kwong LK, Lee EB, Kremmer E, Flatley A, Xu Y, et al.
745 Phosphorylation of S409/410 of TDP-43 is a consistent feature in all sporadic

746 and familial forms of TDP-43 proteinopathies. Acta Neuropathol.
747 2009;117(2):137–49.
748 52. Luisier F, Vonesch C, Blu T, Unser M. Fast interscale wavelet denoising of
749 Poisson-corrupted images. Signal Processing. 2010;90(2):415–27.
750 10.1016/j.sigpro.2009.07.009
751 53. Henden L, Wakeham D, Bahlo M. XIBD: software for inferring pairwise
752 identity by descent on the X chromosome. Bioinformatics. 2016 Aug
753 1;32(15):2389–91. 10.1093/bioinformatics/btw124
754 54. Li H, Glusman G, Hu H, Shankaracharya, Caballero J, Hubley R, et al.
755 Relationship Estimation from Whole-Genome Sequence Data. Visscher PM,
756 editor. PLoS Genet. 2014 Jan 30;10(1):e1004144.
757 10.1371/journal.pgen.1004144
758 55. Brettschneider J, Del Tredici K, Toledo JB, Robinson JL, Irwin DJ, Grossman
759 M, et al. Stages of pTDP-43 pathology in amyotrophic lateral sclerosis. Ann
760 Neurol. 2013 Jul;74(1):20–38. 10.1002/ana.23937
761 56. Mackenzie IRA, Arzberger T, Kremmer E, Troost D, Lorenzl S, Mori K, et al.
762 Dipeptide repeat protein pathology in C9ORF72 mutation cases: clinico-
763 pathological correlations. Acta Neuropathol. 2013 Dec 6;126(6):859–79.
764 10.1007/s00401-013-1181-y
765 57. Gorrie GH, Fecto F, Radzicki D, Weiss C, Shi Y, Dong H, et al. Dendritic
766 spinopathy in transgenic mice expressing ALS/dementia-linked mutant
767 UBQLN2. Proceedings of the National Academy of Sciences. 2014 Oct
768 7;111(40):14524–9. 10.1073/pnas.1405741111
769 58. Ravits J, Appel S, Baloh RH, Barohn R, Rix Brooks B, Elman L, et al.
770 Deciphering amyotrophic lateral sclerosis: What phenotype, neuropathology
771 and genetics are telling us about pathogenesis. Amyotroph Lateral Scler
772 Frontotemporal Degener. 2013 May 16;14(sup1):5–18.
773 10.3109/21678421.2013.778548
774 59. Nguyen HP, Van Broeckhoven C, van der Zee J. ALS Genes in the Genomic
775 Era and their Implications for FTD. Trends in Genetics. 2018;34(6):404–23.
776 10.1016/j.tig.2018.03.001

60. Taylor JP, Brown RH, Cleveland DW. Decoding ALS: from genes to mechanism. Nature. 2016 Nov 9;539(7628):197–206. 10.1038/nature20413
61. Ling S, Polymenidou M, Cleveland DW. Converging Mechanisms in ALS and FTD: Disrupted RNA and Protein Homeostasis. Neuron. 2013 Aug;79(3):416–38. 10.1016/j.neuron.2013.07.033
62. Mori K, Weng S-M, Arzberger T, May S, Rentzsch K, Kremmer E, et al. The C9orf72 GGGGCC Repeat Is Translated into Aggregating Dipeptide-Repeat Proteins in FTLD/ALS. Science (1979). 2013 Mar 15;339(6125):1335–8. 10.1126/science.1232927
63. Mori K, Arzberger T, Grässer FA, Gijselinck I, May S, Rentzsch K, et al. Bidirectional transcripts of the expanded C9orf72 hexanucleotide repeat are translated into aggregating dipeptide repeat proteins. Acta Neuropathol. 2013 Dec 17;126(6):881–93. 10.1007/s00401-013-1189-3
64. Shibata N, Hirano A, Kobayashi M, Siddique T, Deng H-X, Hung W-Y, et al. Intense Superoxide Dismutase-1 Immunoreactivity in Intracytoplasmic Hyaline Inclusions of Familial Amyotrophic Lateral Sclerosis with Posterior Column Involvement. J Neuropathol Exp Neurol. 1996 Apr;55(4):481–90. 10.1097/00005072-199604000-00011
65. Bruijn LI, Houseweart MK, Kato S, Anderson KL, Anderson SD, Ohama E, et al. Aggregation and Motor Neuron Toxicity of an ALS-Linked SOD1 Mutant Independent from Wild-Type SOD1. Science (1979). 1998 Sep 18;281(5384):1851–4. 10.1126/science.281.5384.1851
66. Keith JL, Swinkin E, Gao A, Alminawi S, Zhang M, McGoldrick P, et al. Neuropathologic description of CHCHD10 mutated amyotrophic lateral sclerosis. Neurol Genet. 2020 Feb 13;6(1):e394. 10.1212/NXG.0000000000000394
67. Smith BN, Topp SD, Fallini C, Shibata H, Chen H-J, Troakes C, et al. Mutations in the vesicular trafficking protein annexin A11 are associated with amyotrophic lateral sclerosis. Sci Transl Med. 2017 May 3;9(388):eaad9157. 10.1126/scitranslmed.aad9157

807 68. Smith BN, Vance C, Scotter EL, Troakes C, Wong CH, Topp S, et al. Novel
808 mutations support a role for Profilin 1 in the pathogenesis of ALS. Neurobiol
809 Aging. 2015;36(3):1602.e17-1602.e27. 10.1016/j.neurobiolaging.2014.10.032
810 69. Teyssou E, Takeda T, Lebon V, Boillée S, Doukouré B, Bataillon G, et al.
811 Mutations in SQSTM1 encoding p62 in amyotrophic lateral sclerosis: genetics
812 and neuropathology. Acta Neuropathol. 2013 Apr 17;125(4):511–22.
813 10.1007/s00401-013-1090-0
814 70. Hirsch-Reinshagen V, Pottier C, Nicholson AM, Baker M, Hsiung G-YR,
815 Krieger C, et al. Clinical and neuropathological features of ALS/FTD with
816 TIA1 mutations. Acta Neuropathol Commun. 2017 Dec 7;5(1):96.
817 10.1186/s40478-017-0493-x
818 71. Tada M, Doi H, Koyano S, Kubota S, Fukai R, Hashiguchi S, et al. Matrin 3 Is
819 a Component of Neuronal Cytoplasmic Inclusions of Motor Neurons in
820 Sporadic Amyotrophic Lateral Sclerosis. American Journal of Pathology.
821 2018;188(2):507–14. 10.1016/j.ajpath.2017.10.007
822 72. van Deerlin VM, Leverenz JB, Bekris LM, Bird TD, Yuan W, Elman LB, et al.
823 TARDBP mutations in amyotrophic lateral sclerosis with TDP-43
824 neuropathology: a genetic and histopathological analysis. Lancet Neurol. 2008
825 May;7(5):409–16. 10.1016/S1474-4422(08)70071-1
826 73. Tan RH, Kril JJ, Fatima M, McGeachie A, McCann H, Shepherd C, et al. TDP-
827 43 proteinopathies: pathological identification of brain regions differentiating
828 clinical phenotypes. Brain. 2015 Oct;138(10):3110–22. 10.1093/brain/awv220
829 74. McEachin ZT, Gendron TF, Raj N, García-Murias M, Banerjee A, Purcell RH,
830 et al. Chimeric Peptide Species Contribute to Divergent Dipeptide Repeat
831 Pathology in c9ALS/FTD and SCA36. Neuron. 2020 Jul;107(2):292-305.e6.
832 10.1016/j.neuron.2020.04.011
833 75. Freibaum BD, Taylor JP. The Role of Dipeptide Repeats in C9ORF72-Related
834 ALS-FTD. Front Mol Neurosci. 2017 Feb 13;10(February):1–9.
835 10.3389/fnmol.2017.00035
836 76. Lee Y-B, Baskaran P, Gomez-Deza J, Chen H-J, Nishimura AL, Smith BN, et
837 al. C9orf72 poly GA RAN-translated protein plays a key role in amyotrophic

838 lateral sclerosis via aggregation and toxicity. Hum Mol Genet. 2017 Dec
839 15;26(24):4765–77. 10.1093/hmg/ddx350
840 77. Nonaka T, Masuda-Suzukake M, Hosokawa M, Shimozawa A, Hirai S, Okado
841 H, et al. C9ORF72 dipeptide repeat poly-GA inclusions promote intracellular
842 aggregation of phosphorylated TDP-43. Hum Mol Genet. 2018 Aug
843 1;27(15):2658–70. 10.1093/hmg/ddy174
844 78. Lindsay RD, Scheibel AB. Quantitative analysis of dendritic branching pattern
845 of granular cells from human dentate gyrus. Exp Neurol. 1976 Aug;52(2):295–
846 310. 10.1016/0014-4886(76)90173-4
847 79. Amaral DG, Scharfman HE, Lavenex P. The dentate gyrus: fundamental
848 neuroanatomical organization (dentate gyrus for dummies). In: Prog Brain Res.
849 2007. p. 3–790. 10.1016/S0079-6123(07)63001-5
850 80. May S, Hornburg D, Schludi MH, Arzberger T, Rentzsch K, Schwenk BM, et
851 al. C9orf72 FTLD/ALS-associated Gly-Ala dipeptide repeat proteins cause
852 neuronal toxicity and Unc119 sequestration. Acta Neuropathol. 2014 Oct
853 14;128(4):485–503. 10.1007/s00401-014-1329-4
854 81. Gupta R, Lan M, Mojsilovic-Petrovic J, Choi WH, Safren N, Barmada S, et al.
855 The Proline/Arginine Dipeptide from Hexanucleotide Repeat Expanded
856 C9ORF72 Inhibits the Proteasome. eNeuro. 2017 Jan;4(1):ENEURO.0249-
857 16.2017. 10.1523/ENEURO.0249-16.2017
858 82. Zhang Y-J, Gendron TF, Grima JC, Sasaguri H, Jansen-West K, Xu Y-F, et al.
859 C9ORF72 poly(GA) aggregates sequester and impair HR23 and
860 nucleocytoplasmic transport proteins. Nat Neurosci. 2016 May 21;19(5):668–
861 77. 10.1038/nn.4272
862 83. van Blitterswijk M, Gendron TF, Baker MC, DeJesus-Hernandez M, Finch
863 NA, Brown PH, et al. Novel clinical associations with specific C9ORF72
864 transcripts in patients with repeat expansions in C9ORF72. Acta Neuropathol.
865 2015 Dec 5;130(6):863–76. 10.1007/s00401-015-1480-6
866 84. Webster CP, Smith EF, Bauer CS, Moller A, Hautbergue GM, Ferraiuolo L, et
867 al. The C9orf72 protein interacts with Rab1a and the <scp>ULK</scp> 1

868 complex to regulate initiation of autophagy. EMBO J. 2016 Aug
869 22;35(15):1656–76. 10.15252/embj.201694401
870 85. Wang M, Wang H, Tao Z, Xia Q, Hao Z, Prehn JHM, et al. C9orf72 associates
871 with inactive Rag GTPases and regulates mTORC1-mediated autophagosomal
872 and lysosomal biogenesis. Aging Cell. 2020 Apr 25;19(4):1–14.
873 10.1111/acel.13126
874 86. Boivin M, Pfister V, Gaucherot A, Ruffenach F, Negroni L, Sellier C, et al.
875 Reduced autophagy upon C9ORF72 loss synergizes with dipeptide repeat
876 protein toxicity in G4C2 repeat expansion disorders. EMBO J. 2020 Feb
877 17;39(4):1–15. 10.15252/embj.2018100574
878 87. Zhu Q, Jiang J, Gendron TF, McAlonis-Downes M, Jiang L, Taylor A, et al.
879 Reduced C9ORF72 function exacerbates gain of toxicity from ALS/FTD-
880 causing repeat expansion in C9orf72. Nat Neurosci. 2020;23(May).
881 10.1038/s41593-020-0619-5
882 88. Beckers J, Tharkeshwar AK, van Damme P. C9orf72 ALS-FTD: recent
883 evidence for dysregulation of the autophagy-lysosome pathway at multiple
884 levels. Autophagy. 2021;00(00):1–17. 10.1080/15548627.2021.1872189
885 89. Sellier C, Campanari M, Julie Corbier C, Gaucherot A, Kolb-Cheynel I, Oulad-
886 Abdelghani M, et al. Loss of C9ORF72 impairs autophagy and synergizes with
887 polyQ Ataxin-2 to induce motor neuron dysfunction and cell death. EMBO J.
888 2016 Jun 15;35(12):1276–97. 10.15252/embj.201593350
889 90. Renaud L, Picher-Martel V, Codron P, Julien J. Key role of UBQLN2 in
890 pathogenesis of amyotrophic lateral sclerosis and frontotemporal dementia.
891 Acta Neuropathol Commun. 2019 Dec 18;7(1):103. 10.1186/s40478-019-
892 0758-7
893 91. Zhang KY, Yang S, Warraich ST, Blair IP. Ubiquilin 2: A component of the
894 ubiquitin-proteasome system with an emerging role in neurodegeneration.
895 International Journal of Biochemistry and Cell Biology. 2014;50(1):123–6.
896 10.1016/j.biocel.2014.02.018
897 92. Sharkey LM, Sandoval-Pistorius SS, Moore SJ, Gerson JE, Komlo R, Fischer
898 S, et al. Modeling UBQLN2-mediated neurodegenerative disease in mice:

899 Shared and divergent properties of wild type and mutant UBQLN2 in phase
900 separation, subcellular localization, altered proteostasis pathways, and
901 selective cytotoxicity. Neurobiol Dis. 2020;143(June).
902 93. Mann DM, Rollinson S, Robinson A, Bennion Callister J, Thompson JC,
903 Snowden JS, et al. Dipeptide repeat proteins are present in the p62 positive
904 inclusions in patients with frontotemporal lobar degeneration and motor
905 neurone disease associated with expansions in C9ORF72. Acta Neuropathol
906 Commun. 2013 Dec 14;1(1):68. 10.1186/2051-5960-1-68
907 94. Al-Sarraj S, King A, Troakes C, Smith B, Maekawa S, Bodi I, et al. p62
908 positive, TDP-43 negative, neuronal cytoplasmic and intranuclear inclusions in
909 the cerebellum and hippocampus define the pathology of C9orf72-linked
910 FTLD and MND/ALS. Acta Neuropathol. 2011 Dec 19;122(6):691–702.
911 10.1007/s00401-011-0911-2
912 95. Piras A, Collin L, Grüninger F, Graff C, Rönnbäck A. Autophagic and
913 lysosomal defects in human tauopathies: analysis of post-mortem brain from
914 patients with familial Alzheimer disease, corticobasal degeneration and
915 progressive supranuclear palsy. Acta Neuropathol Commun. 2016;4:22.
916 10.1186/s40478-016-0292-9
917 96. Babu JR, Geetha T, Wooten MW. Sequestosome 1/p62 shuttles
918 polyubiquitinated tau for proteasomal degradation. J Neurochem. 2005
919 Jul;94(1):192–203. 10.1111/j.1471-4159.2005.03181.x
920 97. Zatloukal K, Stumptner C, Fuchsbichler A, Heid H, Schnoelzer M, Kenner L,
921 et al. P62 Is a Common Component of Cytoplasmic Inclusions in Protein
922 Aggregation Diseases. American Journal of Pathology. 2002;160(1):255–63.
923 10.1016/S0002-9440(10)64369-6
924 98. Kuusisto E, Salminen A, Alafuzoff I. Ubiquitin-binding protein p62 is present
925 in neuronal and glial inclusions in human tauopathies and synucleinopathies.
926 Neuroreport. 2001 Jul;12(10):2085–90. 10.1097/00001756-200107200-00009
927 99. Richards S, Aziz N, Bale S, Bick D, Das S, Gastier-Foster J, et al. Standards
928 and guidelines for the interpretation of sequence variants: a joint consensus
929 recommendation of the American College of Medical Genetics and Genomics

930 and the Association for Molecular Pathology. Genetics in Medicine. 2015
931 May;17(5):405–24. 10.1038/gim.2015.30
932 100. Ramstetter MD, Dyer TD, Lehman DM, Curran JE, Duggirala R, Blangero J,
933 et al. Benchmarking relatedness inference methods with genome-wide data
934 from thousands of relatives. Genetics. 2017;207(1):75–82.
935
936

937 ## Tables

938 **Table 1.** IBD segments inferred over *UBQLN2* on the X chromosome (chromosome 23).

939

Individual 1		Individual 2					
Family ID	**Pedigree ID**	**Family ID**	**Individual ID**	**StartSNP**	**EndSNP**	**Start Pos(bp)**	**End Pos(bp)**
FALS5	III:8	FALS5	IV:9	rs17330993	rs11156600	2779749	154440161
FALS5	III:8	FALS5	IV:18[a]	rs7062445	rs6423133	19650411	123608292
FALS5	III:8	FALS14	III:2	rs952836	rs17315029	40344087	129605268
FALS5	IV:9	FALS5	IV:18	rs6628597	rs6423133	31382037	123608292
FALS5	IV:9	FALS14	III:2	rs952836	rs17277770	40344087	132774456
FALS5	IV:18	FALS14	III:2	rs952836	rs6423133	40344087	123608292

940 [a] FALS5 IV:18 is referred to as MN17 in this report.

941

942 **Table 2.** Estimated degree of relatedness and fraction of genome with zero, one, and two
943 alleles identical-by-descent (IBD) between all samples in *UBQLN2* p.T487I-linked
944 families FALS5 and FALS14.
945

	Individual 1		Individual 2					
	Family ID	**Pedigree ID**	**Family ID**	**Individual ID**	**Fraction IBD=0**	**Fraction IBD=1**	**Fraction IBD=2**	**Degree[a]**
Intra-family	FALS5	III:8	FALS5	IV:9	0.529	0.471	0	2
	FALS5	III:8	FALS5	IV:18[b]	0.529	0.471	0	2
	FALS5	IV:9	FALS5	IV:18	0.751	0.249	0	3
	FALS14	II:1	FALS14	III:2	0.515	0.485	0	2
Inter-family	FALS5	III:8	FALS14	II:1	0.877	0.123	0	4
	FALS5	III:8	FALS14	III:2	0.927	0.073	0	5
	FALS5	IV:9	FALS14	II:1	0.942	0.058	0	5
	FALS5	IV:9	FALS14	III:2	0.948	0.052	0	5
	FALS5	IV:18	FALS14	II:1	0.926	0.074	0	5
	FALS5	IV:18	FALS14	III:2	0.948	0.052	0	5

946 [a] Degrees of relatedness as per [100]:
947 2 – Grandparent-grandchild, Avuncular, Half-sibling
948 3 – First cousin, Great-grandparent, Grand-avuncular
949 4 – First cousin once removed, GG-grandparent
950 5 – Second cousin, First cousin twice removed
951 [b] FALS5 IV:18 is referred to as MN17 in this report.

952 ## Figure legends

953 **Figure 1. Ubiquilin 2 labelling in previous studies fails to discriminate between**
954 ***UBQLN2*-linked and other genotypes of ALS/FTD.** Previously published
955 immunohistochemical analyses of hippocampus molecular layer (ML), granule cell layer
956 (GCL), and cornus ammonus (CA) regions fail to discriminate between *UBQLN2*-linked
957 ALS/FTD and ALS/FTD with other genotypes. Key shown within figure. Hippocampal
958 ubiquilin 2 (green) pathology is reported when ubiquilin 2 is either mutant or wildtype;
959 being present in the molecular layer in *UBQLN2*-linked and *C9orf72*-linked ALS/FTD
960 (including "ALS-dementia") but not in sALS; and in the granule cell layer in *C9orf72*-
961 linked ALS/FTD (including "ALS-dementia"). Hippocampal molecular layer ubiquilin 2
962 (green) is frequently reported and found together with ubiquitin (orange) or p62 (beige),
963 but not TDP-43 (blue). Hippocampal granule cell layer ubiquilin 2 pathology is found
964 together with dipeptide repeats (DPRs, pink) with or without TDP-43; but is variably
965 present in *UBQLN2*-linked ALS/FTD and sALS. In the hippocampal CA regions, ubiquilin
966 2 is present in *UBQLN2*-linked and in *C9orf72*-linked ALS/FTD (including "ALS-
967 dementia") where it is found together with DPRs, ubiquitin and p62.
968

969 **Figure 2. Pathology in the hippocampal dentate gyrus and cornu ammonis regions of**
970 **control, familial, and sporadic cases.** The majority of control tissue had no pTDP-43 or
971 ubiquilin 2 pathology, but one case had sparse p62 immunoreactivity in the GCL and CA-
972 pyr layers (**A** H230, pink arrows). Such punctate p62-positive inclusions were also found
973 in the GCL (**B_1-D_1**), and CA-pyr layers (**B_2-D_2**) in MN14, an ALS case of unknown
974 genotypic cause (**B**), MN24, a *SOD1* p.E101G case (**C**), and P525L, a *FUS* p.P525L case
975 (**D**). P62-co-labelled perinuclear pTDP-43 aggregates negative for ubiquilin 2 were found
976 in the GCL and CA-pyr regions of sporadic case ALS/FTD case MN15 (**E_1** and **E_2**, white
977 arrows), and sporadic ALS case MN30 (**F_1** and **F_2**, white arrows). Rare pTDP-43
978 aggregates negative for p62 are indicated by the yellow arrow in **F_2**. Scale bar A-D, 50 µm;
979 E-F, 25 µm. Abbreviations: CA – pyr, cornu ammonis – pyramidal cells; GCL, granule cell
980 layer.
981

982 **Figure 3. Pathology in the hippocampal dentate gyrus and cornu ammonis regions of**
983 ***C9orf72*-linked cases.** Wispy ubiquilin 2 aggregates in the ML and CA – l-m-rad layers
984 were predominantly p62 negative (**A,B$_1$** and **A,B$_2$**, green arrows), with larger aggregates
985 also co-labelling with p62 in the ML (**B$_1$**, white arrow). In MN18, the CA – pyr cells
986 harboured stellate p62 aggregates (**A$_3$**, pink arrow) while the GCL showed stellate p62
987 aggregates either with ubiquilin 2 (**A$_4$**, white arrows) or without (**A$_4$**, pink arrow). Case
988 MN28 shared this pattern of p62 and ubiquilin 2 pathology with the additional presence of
989 perinuclear pTDP-43 inclusions, often found without other co-labelling in the CA-pyr
990 region (**B$_3$**, yellow arrow) and GCL (**B$_4$**, yellow arrow). Ubiquilin 2 aggregates in the ML
991 and CA – l-m/rad layers were negative for dipeptide repeat proteins (**C$_1$-C$_2$**, **D$_1$-D$_2$**, green
992 arrows). The dominant pathology in CA – pyr regions was the presence of polyGA and
993 polyGP inclusions negative for ubiquilin 2 (**C$_3$** and **D$_3$**, orange arrowheads). All GCL
994 ubiquilin 2 was positive for at least one dipeptide repeat protein (**C$_4$** and **D$_4$**, purple arrows).
995 Ubiquilin 2-negative aggregates were comprised of both dipeptide repeat proteins (**C$_4$** and
996 **D$_4$**, orange arrows) or most commonly, polyGA without other co-labelling (**C$_4$** and **D$_4$**, red
997 arrows). Super-resolution STED microscopy of co-localised ubiquilin 2-polyGA GCL
998 aggregates in case MN28 demonstrated polyGA enmeshed with and encircling ubiquilin 2
999 (**E**) or ubiquilin 2 labelling around a core of polyGA (**F**). Scale bar in main images A-D,
1000 50 µm; zooms in C$_4$ and D$_4$, 25 µm; in E-F, 1 µm. Abbreviations: CA – lm/rad, cornu
1001 ammonis – lacunosum-molecular and radiatum layers; CA – pyr, cornu ammonis –
1002 pyramidal cells; GCL, granule cell layer.
1003
1004 **Figure 4. Ubiquilin 2, pTDP-43, and p62 pathology in the hippocampal dentate gyrus**
1005 **and cornu ammonis regions of *UBQLN2*-linked cases.** All *UBQLN2*-linked ALS/FTD
1006 cases showed numerous p62-positive ubiquilin 2 aggregates, indicated by white arrows, in
1007 the ML (**A$_1$-D$_1$**) and CA – l-m/rad layers (**A$_2$-D$_2$**). Case P506S had the additional presence
1008 of aggregates positive for pTDP-43, ubiquilin 2, and p62 in the CA – pyr layer (**D$_2$**, filled
1009 white arrowhead). Cases P497H and MN17-T487I showed no aggregate labelling in the
1010 GCL (**A$_3$**, **B$_3$**). ALS/FTD cases V:7 – T487I and P506S showed rare GCL p62-positive
1011 pTDP-43 aggregates negative for ubiquilin 2 (**C$_3$**, **D$_3$**, hollow white arrowheads). Only in
1012 P506S were the numerous compact pTDP-43 aggregates found in the GCL co-localised

1013 with ubiquilin 2 and p62 (**D3**, filled white arrowheads). A PSP case harbouring a *UBQLN2*
1014 p.S222G variant of uncertain significance (VOUS) (**E**) had pathology in the ML (**E1**), and
1015 sparse p62 positivity (pink arrows) in the CA – lm/rad layers (**E2**) and GCL (**E3**). Scale bar
1016 in main images, 25 µm; zooms, 5 µm. Abbreviations: CA – lm/rad, cornu ammonis –
1017 lacunosum-molecular and radiatum layers; CA – pyr, cornu ammonis – pyramidal cells;
1018 GCL, granule cell layer; PSP, progressive supranuclear palsy.
1019
1020 **Figure 5. Combined pTDP-43, ubiquilin 2, p62, and dipeptide repeat protein**
1021 **immunohistochemical staining discriminated between sporadic, *C9orf72*-linked, and**
1022 ***UBQLN2*-linked ALS/FTD.** Key shown within figure. P62 aggregates ('+' symbol on
1023 brown box) without other co-labelling were observed in CA – pyr and GCL cells in a subset
1024 of neurologically normal controls (n=1 of 5), unrelated familial ALS (n=5 of 5), and
1025 sporadic ALS cases (n=4 of 20). In contrast, pTDP-43 pathology (boxed '+' symbol on
1026 blue box) was present in these layers in a separate subset of sALS cases (n=6 of 20), co-
1027 localising with p62. Ubiquilin 2 pathology ('+' symbol on green box) was present in the
1028 hippocampus when ubiquilin 2 was wildtype (*C9orf72*-linked ALS) or mutant (*UBQLN2*-
1029 linked ALS/FTD). Wildtype ubiquilin 2 in *C9orf72*-linked ALS ML and CA – lm/rad
1030 regions was p62-negative, and in the CA – pyr layer was associated with polyGA, polyGP,
1031 and p62 aggregates. PolyGA and polyGP aggregates were found in the GCL with or
1032 without ubiquilin 2, all colocalising with p62. CA – pyr and GCL aggregates had additional
1033 pTDP-43 pathology in only one case, and even then, only rarely. Mutant ubiquilin 2
1034 aggregates in *UBQLN2*-linked ALS/FTD ML, and CA – lm/rad regions were p62-positive
1035 and associated with GCL pTDP-43 aggregates only in some cases and either with or
1036 without ubiquilin 2 co-labelling. Blue outlines indicate unique aggregation features of
1037 *C9orf72*-linked ALS and *UBQLN2*-linked ALS/FTD hippocampal pathology.
1038 Abbreviations: CA – lm/rad, cornu ammonis – lacunosum-molecular and radiatum layers;
1039 CA – pyr, cornu ammonis – pyramidal cells; GCL, granule cell layer.
1040
1041 **Figure 6. Schematic representation of the hippocampal neuropathological signature**
1042 **defining *UBQLN2*-linked ALS/FTD.** In *UBQLN2*-linked ALS/FTD cases without
1043 hippocampal pTDP-43 proteinopathy, mutant ubiquilin 2 is punctate, p62-positive, and

1044 forms aggregates exclusively in the CA l-m/rad layer and ML (cases p.P497H and MN17
1045 – p.T487I). In *UBQLN2*-linked ALS/FTD cases with hippocampal pTDP-43
1046 proteinopathy, in addition to punctate p62-positive ubiquilin 2 aggregates in the CA l-
1047 m/rad, and molecular layers, there are granule cell layer pTDP-43 aggregates that are
1048 either; frequent and ubiquilin 2-labelled (case p.P506S), or rare and ubiquilin 2-negative
1049 (case V7-p.T487I), suggesting a pathological cascade in which granule cell layer pTDP-43
1050 aggregates provide a scaffold around which mutant ubiquilin 2 can aggregate.
1051 Abbreviations: CA – lm/rad, cornu ammonis – lacunosum-molecular and radiatum layers;
1052 CA – pyr, cornu ammonis – pyramidal cells; GCL, granule cell layer. Image created in
1053 Biorender.com

	Hippocampal formation		
***UBQLN2*-linked ALS/FTD**	**ML**	**GCL**	**CA regions**
Deng et al., 2011; ***P506T***	+ □ + □ □ □	− □ ■ □ □ □	+ □ + □ □ □
Gkazi et al, 2019; ***P506S***	■ □ ■ □ □ □	+ + ■ □ □ □	■ □ ■ □ □ □
Wu et al, 2020; ***P506S***	+ □ ■ + □ □	■ □ ■ □ □ □	■ □ ■ □ □ □
Wu et al, 2020; ***P497H***	+ □ ■ + □ □	■ □ ■ □ □ □	■ □ ■ □ □ □
Fahed et al, 2014; ***P497L***	+ □ ■ □ □ □	− □ ■ □ □ □	■ □ ■ □ □ □
Scotter et al, 2017; ***T487I***	+ − ■ □ − □	− − ■ □ − □	■ □ ■ □ □ □
Wu et al, 2020; ***T487I***	+ □ ■ + □ □	■ □ ■ □ □ □	■ □ ■ □ □ □
Williams et al, 2012; ***T487I***	■ □ ■ □ □ □	■ □ ■ □ □ □	■ □ ■ □ □ □
Non *UBQLN2*-linked ALS/FTD			
Deng et al, 2011; ***ALS-dementia****	+ − + □ □ −	+ + + + □ −	+ − + + □ □
Brettschneider et al, 2012; ***C9orf72***	+ − ■ + − □	+ + ■ □ + □	+ □ ■ □ + □
Brettschneider et al, 2012; Non-***C9orf72***	■ □ ■ □ □ □	+ + ■ □ □ □	■ □ ■ □ □ □
Scotter et al, 2017; ***C9orf72***	+ − ■ □ □ □	+ − ■ □ + □	+ □ ■ □ + □
Scotter et al, 2017; ***sALS***	− − ■ □ − □	− − ■ □ − □	■ □ ■ □ □ □
Gkazi et al, 2019; ***sALS***	■ □ ■ □ □ □	+ □ ■ □ □ □	■ □ ■ □ □ □

* *C9ORF72*-linked

Key

□ TDP-43 ■ Ubiquilin 2 ■ Ubiquitin □ p62 □ Dipeptide repeat proteins □ FUS

ML Molecular layer **GCL** Granule cell layer **CA** Cornu ammonis

\+ Presence of pathology − Absence of pathology **sALS** sporadic amyotrophic lateral sclerosis

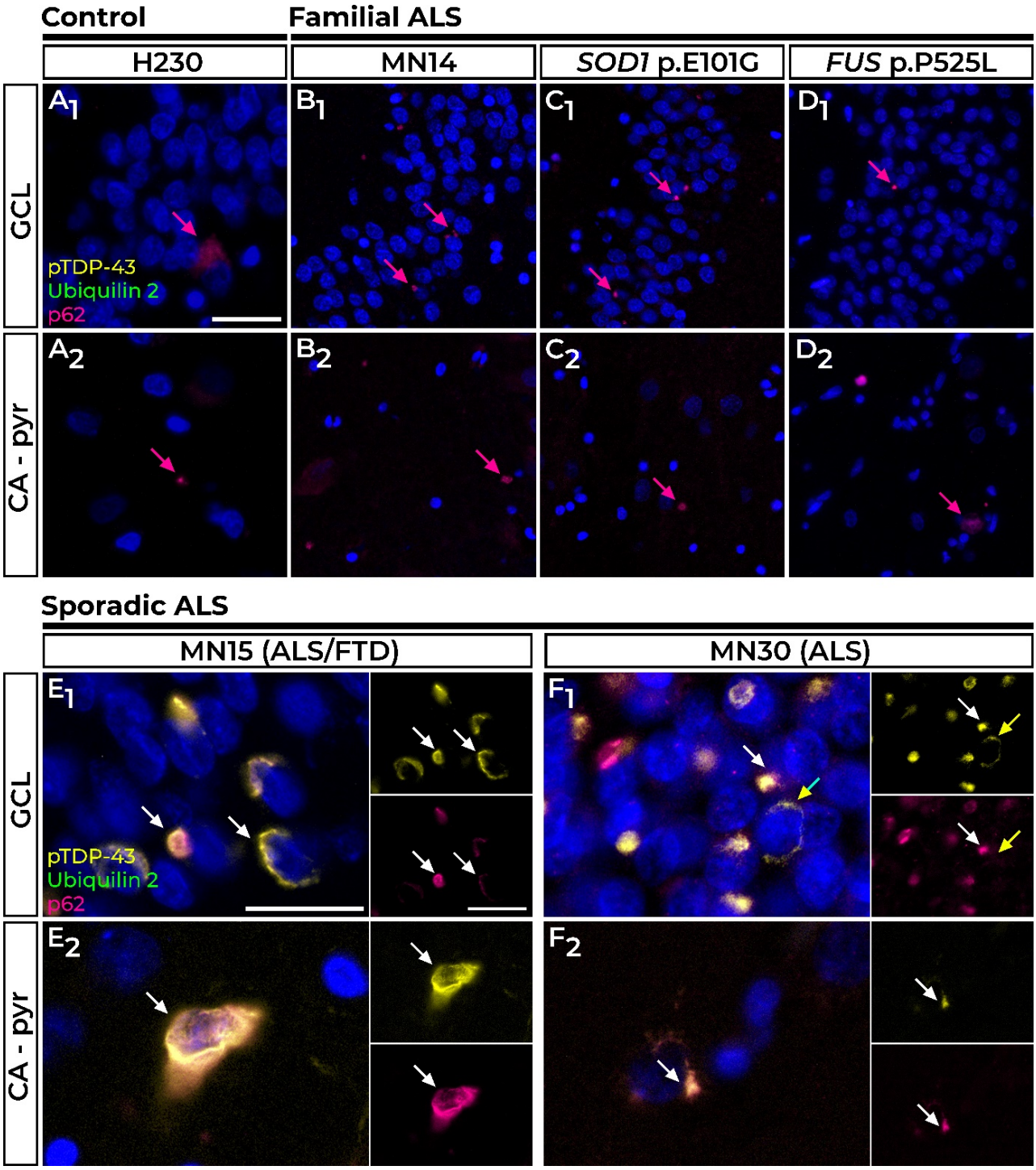
Control
Familial ALS
H230
MN14
SOD1 p.E101G
FUS p.P525L
GCL
CA - pyr
A1
B1
C1
D1
A2
B2
C2
D2
pTDP-43
Ubiquilin 2
p62
Sporadic ALS
MN15 (ALS/FTD)
MN30 (ALS)
E1
F1
E2
F2

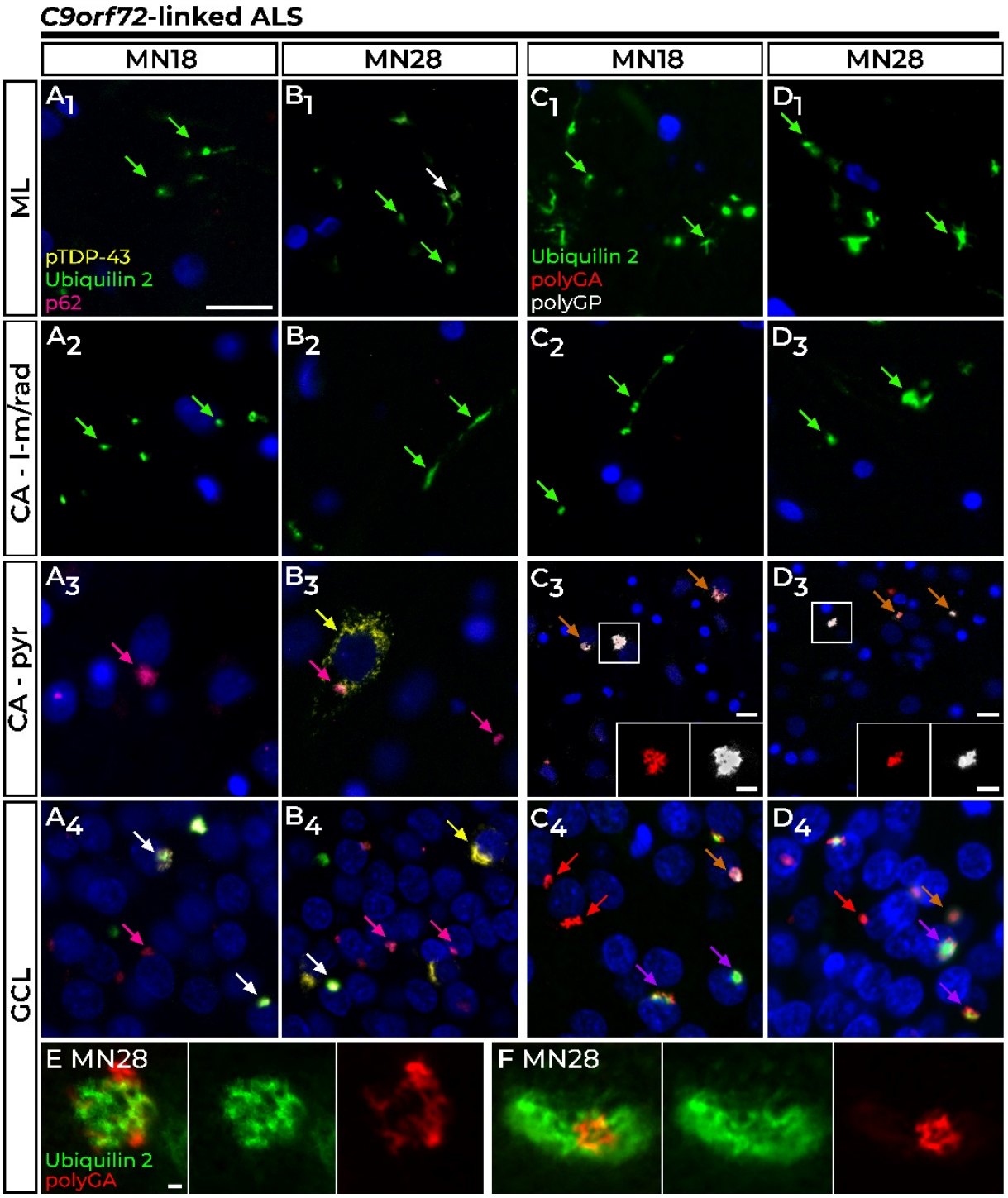
C9orf72-linked ALS
MN18
MN28
MN18
MN28
ML
CA - l-m/rad
CA - pyr
GCL
A1
B1
C1
D1
pTDP-43
Ubiquilin 2
p62
Ubiquilin 2
polyGA
polyGP
A2
B2
C2
D3
A3
B3
C3
D3
A4
B4
C4
D4
E MN28
Ubiquilin 2
polyGA
F MN28

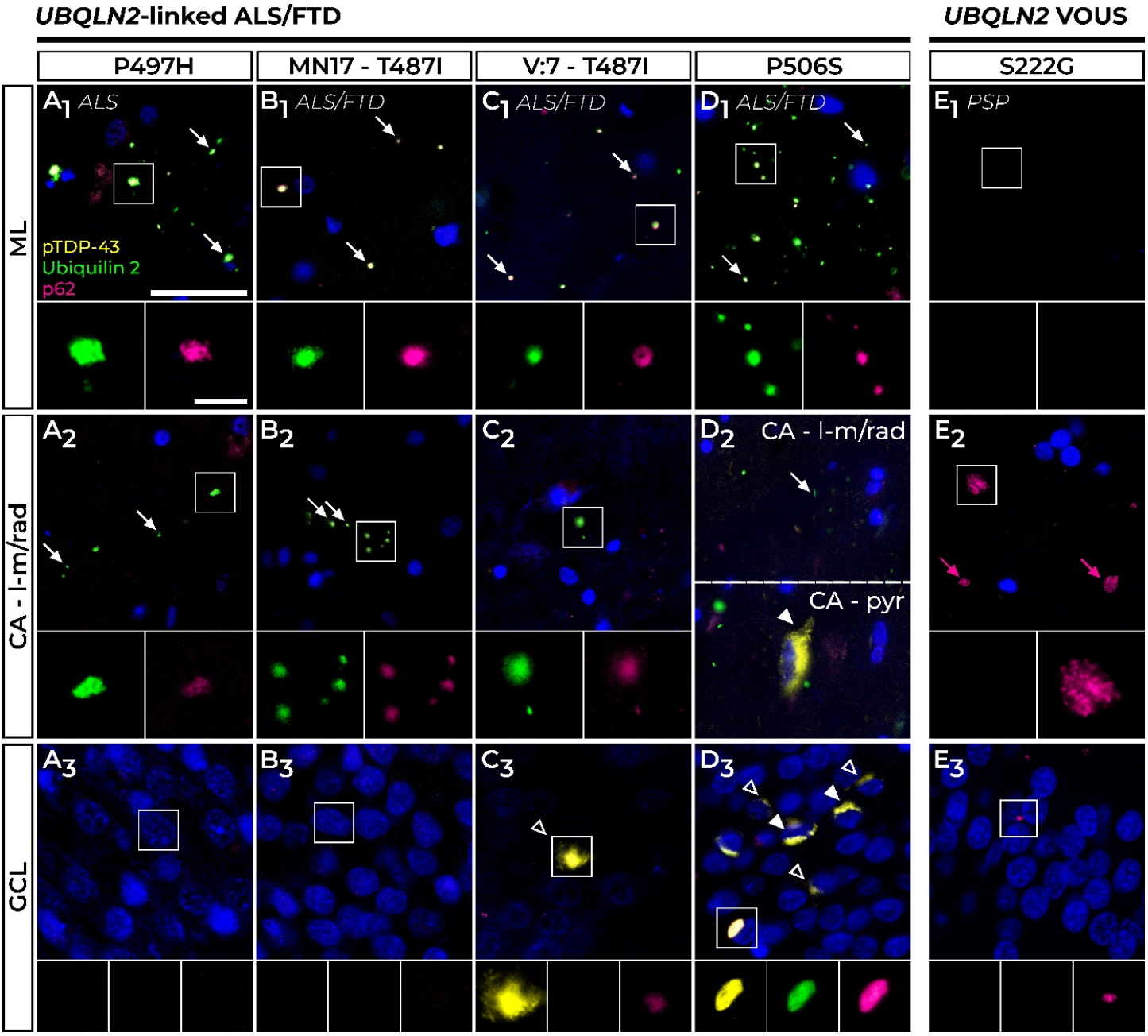
UBQLN2-linked ALS/FTD
UBQLN2 VOUS
P497H
MN17 - T487I
V:7 - T487I
P506S
S222G
ML
CA - l-m/rad
GCL
A1 ALS
B1 ALS/FTD
C1 ALS/FTD
D1 ALS/FTD
E1 PSP
pTDP-43
Ubiquilin 2
p62
A2
B2
C2
D2 CA - l-m/rad
CA - pyr
E2
A3
B3
C3
D3
E3

Genetic classification	Case	Diagnosis	Aggregate deposition			
			ML	CA - l-m/rad	CA - pyr	GCL
Control (n=5)		Neurologically normal				
Control (n=1)	H230	Neurologically normal			+	+
Familial ALS (n=5)					+	+
Sporadic ALS (n=10)						
Sporadic ALS (n=4)					+	+
Sporadic ALS (n=6)	MN27	MND-ALS/LBD				+ +
	MN19	MND-ALS			+ +	+ +
	MN13	MND-ALS			+ +	+ +
	MN29	MND-ALS			+ +	+ +
	MN15	MND-ALS/FTD			+ +	+ +
	MN30	MND-ALS			+ +	+ +
C9orf72-linked ALS (n=5)	MN2	MND-ALS	+	+	+ + +	+ + + +
	MN18	MND-ALS	+	+	+ + +	+ + + +
	MN23	MND-ALS	+	+	+ + +	+ + + +
	MN33	MND-ALS	+	+	+ + +	+ + + +
	MN28	MND-ALS	+	+	+ + +	+ + + +
UBQLN2-linked VOUS (n=1)	S222G	PSP	+		+	
UBQLN2-linked ALS/FTD (n=4)	P497H	MND-ALS	+ +	+ +		
	MN17 - T487I	MND-ALS/FTD	+ +	+ +		
	V:7 - T487I	MND-ALS/FTD	+ +	+ +		+
	P506S	MND-ALS/FTD	+ +	+ +	+ + +	+ + +

Key **ML** Molecular layer **GCL** Granular cell layer **CA - l-m/rad** Cornu ammonis lacunosum-molecular and radiatum layer **CA - pyr** Cornu ammonis pyramidal layer

pTDP-43 Ubiquilin 2 p62 polyGA polyGP + Presence of pathology − Absence of pathology Stage 4 ALS Protein signature

LBD Lewy body dementia **FTD** Frontotemporal dementia **PSP** Progressive supranuclear palsy **VOUS** Variant of uncertain significance

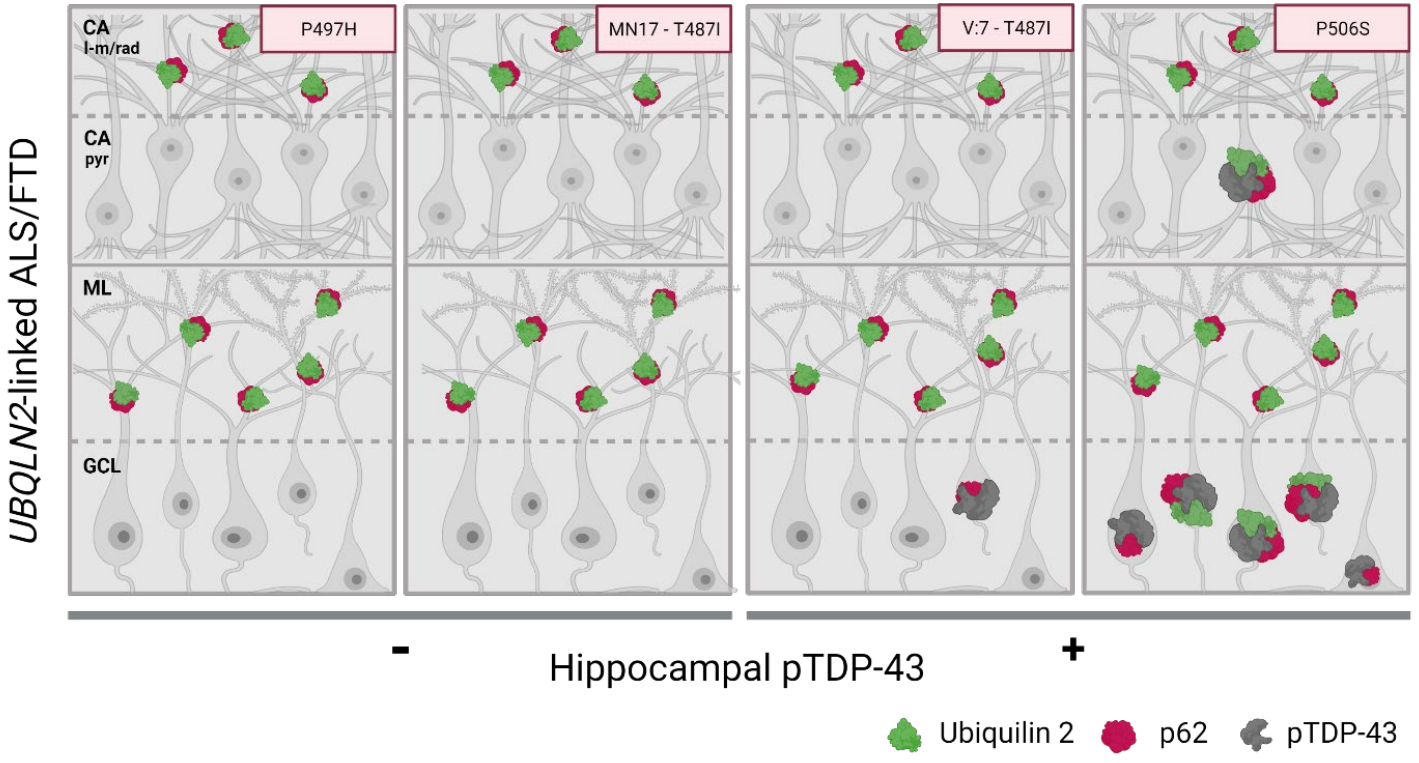
UBQLN2-linked ALS/FTD
CA
l-m/rad
CA
pyr
ML
GCL
P497H
MN17 - T487I
V:7 - T487I
P506S
-
+
Hippocampal pTDP-43
Ubiquilin 2
p62
pTDP-43